microbiology research

MDPI

Article

Biothermodynamic Analysis of Norovirus: Mechanistic Model of Virus–Host Interactions and Virus–Virus Competition Based on Gibbs Energy

Marko E. Popović [1,*], Vojin Tadić [2] and Marijana Pantović Pavlović [1,3]

[1] Institute of Chemistry, Technology and Metallurgy, University of Belgrade, Njegoševa 12, 11000 Belgrade, Serbia; m.pantovic@ihtm.bg.ac.rs
[2] Department for Experimental Testing of Precious Metals, Mining and Metallurgy Institute, Zeleni Bulevar 35, 19210 Bor, Serbia; vojintadic@yahoo.com
[3] Centre of Excellence in Chemistry and Environmental Engineering—ICTM, University of Belgrade, 11000 Belgrade, Serbia
* Correspondence: marko.popovic@ihtm.bg.ac.rs

Abstract: Norovirus is a leading cause of viral gastroenteritis worldwide and has been studied extensively from the perspective of life and biomedical sciences. However, no biothermodynamic analysis of Norovirus has been reported in the literature. Such an analysis would provide insights into the role of energetic constraints in the interactions between Norovirus and its host cells and other viruses. In this research, Norovirus was characterized from the aspect of chemistry and chemical thermodynamics, with the determination of its molecular formula, empirical formula, molar mass and thermodynamic properties (enthalpy, entropy, Gibbs energy) of formation. Based on these properties, biosynthesis reactions were formulated that show how Norovirus particles are synthetized inside host cells, and the thermodynamic properties of biosynthesis were determined. Moreover, the thermodynamic properties of the binding of Norovirus to its host cell receptor were determined. These were then used to develop a model of virus–host interactions at the cell membrane (antigen-receptor binding) and inside the cytoplasm (virus multiplication), with the phenomenological equations of nonequilibrium thermodynamics. Based on the model, an analysis of the virus–virus competition between Norovirus and Rotavirus was conducted.

Keywords: antigen-receptor binding; virus multiplication; infectivity; pathogenicity; epidemic; driving force

check for updates

Academic Editor: Takayuki Murata

Received: 8 April 2025
Revised: 28 May 2025
Accepted: 30 May 2025
Published: 1 June 2025

Citation: Popović, M.E.; Tadić, V.; Pantović Pavlović, M. Biothermodynamic Analysis of Norovirus: Mechanistic Model of Virus–Host Interactions and Virus–Virus Competition Based on Gibbs Energy. *Microbiol. Res.* **2025**, *16*, 112. https://doi.org/10.3390/microbiolres16060112

Copyright: © 2025 by the authors. Licensee MDPI, Basel, Switzerland. This article is an open access article distributed under the terms and conditions of the Creative Commons Attribution (CC BY) license (https://creativecommons.org/licenses/by/4.0/).

1. Introduction

Norovirus is a major cause of viral gastroenteritis worldwide [1,2]. It belongs to Noroviruses (NoVs), which are emerging pathogens that represent a risk for human health [3]. Norovirus has been studied extensively from the perspective of life and biomedical sciences. However, in the literature, no study of Norovirus was reported from the perspective of biothermodynamics. The biothermodynamic approach has been applied to research on several viruses, which include SARS-CoV-2 [4–8], SARS-CoV [9], MERS-CoV [10], Ebola [11], Rhinovirus [12], Mpox [13], Rotavirus [14], HIV [15], Dengue virus [16], West Nile virus [17], Arboviruses [15,18,19], Coxsackievirus [20], etc. This research was able to explain interactions between viruses and their host organisms at the cell membrane (virus attachment and entry into host cells) [12,21,22] and in the cytoplasm (virus multiplication) [4,7,23]. Biothermodynamics was applied in studies of interactions between viruses and evolution of viruses [4,24,25]. Moreover, a biothermodynamic methodology

was used to analyze the development of epidemics and pandemics [6,26]. This is why a biothermodynamic analysis could provide insights into the role of the metabolic energy requirements in interactions between Norovirus and its host cells and other viruses.

Viruses lack cellular metabolic machinery and must therefore hijack the metabolism of a host cell in order to multiply [27–29]. They have been studied extensively from the perspective of life and biomedical sciences [30–32]. With the development of biology and chemistry, the approach of molecular biology and biochemistry have contributed greatly to our understanding of viruses [33–35]. Genetic and protein sequences have been determined for many viruses [36–38]. Moreover, interactions of viruses with their host cells have been studied extensively at the molecular level in molecular virology [39–41].

Except for biological systems, viruses also represent macromolecular assemblies and can therefore be analyzed as chemical and thermodynamic systems [24,42,43]. Inside host cells, viruses establish metabolic processes [44–46]. These include replication, transcription, translation, and self-assembly processes [47–49]. All these processes represent chemical reactions [50–52]. These reactions can be analyzed with the methodology of chemical thermodynamics [53–55]. This approach can provide insight into energetic constraints on metabolic processes in biological systems [56–58].

Based on genetic and protein sequences, chemical and thermodynamic properties of viruses can be found [7,59,60]. The approach of chemical thermodynamics can be a useful tool in studies of virus–host interactions, which can complement the approaches of molecular biology and biochemistry [61–65]. Biothermodynamics was applied to study interactions between organisms [66,67] and evolution [68,69]. It has been applied in research on competition between the variants of SARS-CoV-2 [21,70,71]. Moreover, biothermodynamics was applied in studies on virus–host interactions [5,8,23] and epidemiology [6,26]. It has been applied in research on virus–virus competition [21,70]. The biothermodynamic approach can provide additional information about virus–host interactions, based on the results of molecular biology and biochemistry.

Norovirus, also known as Norwalk virus, belongs to the *Caliciviridae* family [72,73]. In humans, it causes acute gastroenteritis known as the winter vomiting disease [74,75]. Norovirus is primarily transmitted by the fecal–oral route, which includes direct person-to-person contact, contact with contaminated surfaces, ingestion of contaminated water or food and aerosol transmission [76,77]. Norovirus can cause infection with a very small infective inoculum, which means that only a very small number of virions are required for infection [78,79]. This makes Norovirus highly contagious [80,81] and its epidemics difficult to control [82,83]. The incubation period is 12 to 48 h [84,85]. The symptoms include diarrhea, vomiting, nausea, stomach pain, and sometimes fever, headache and body aches [84,85].

Norovirus has an unsegmented single-stranded positive-sense RNA genome [86–89]. Norovirus particles are non-enveloped [90–93]. Most Norovirus virions are of T = 3 icosahedral symmetry [94–97]. They are composed of the RNA genome and 180 copies of the VP1 capsid protein [98–101]. The VP1 capsid proteins are arranged as 90 dimers [102–105]. The VP1 capsid protein contains the shell (S) and protruding (P) domains [106,107]. The S domain forms the interior shell of the capsid [108,109]. The P domain consists of the P1 and P2 subdomains [110,111]. The P2 subdomain represents the viral antigen that binds to the host cell receptor [112–115]. After antigen-receptor binding, the virus enters the cell by endocytosis [116–119].

The goal of this paper is to perform a chemical and thermodynamic analysis of Norovirus. This was carried out by determining its molecular formula, empirical formula, thermodynamic properties (enthalpy, entropy, and Gibbs energy) of formation, biosynthesis reactions, and thermodynamic properties of biosynthesis. These properties were used to

develop a mechanistic model of virus–host interaction of Norovirus with its host enterocytes. Based on the model, virus–virus interactions between Norovirus and Rotavirus were discussed.

2. Methods

2.1. Data Sources

The genetic sequence and sequence of the VP1 capsid protein of the Norovirus strain GII was taken from the NCBI database [120,121]. The genetic sequence can be found under the accession number NC_044932.1 [122] and is reported by [123]. The sequence of the VP1 capsid protein can be found under the accession number AIV43156.2 [124] and is reported by [125]. The Norovirus capsid exhibits T = 3 icosahedral symmetry and consists of 180 copies of the VP1 capsid protein [126,127].

Dissociation equilibrium constant, K_d, data for the binding of the VP1 protruding (P) domain of Murine norovirus (MNoV) to the CD300lf receptor were taken from [128,129]. They were measured through surface plasmon resonance (SPR) and isothermal titration calorimetry (ITC) at 25 °C [128]. The dissociation equilibrium constant for the binding of Norovirus VP1 P domain to the CD300lf receptor in absence of Ca^{2+}, Mg^{2+} and GCDCA (glycochenodeoxycholic acid) is K_d = 219 μM [128,129]. The dissociation equilibrium constant for the binding of the Norovirus VP1 P domain to the CD300lf receptor in the presence of Ca^{2+} ions is K_d = 24.51 μM [128]. The dissociation equilibrium constant for the binding of Norovirus VP1 P domain to the CD300lf receptor in the presence of Mg^{2+} ions and EGTA (ethylene glycol-bis(β-aminoethyl ether)-*N*,*N*,*N*′,*N*′-tetraacetic acid) is K_d = 24.29 μM [128]. The dissociation equilibrium constant for binding of Norovirus VP1 P domain to the CD300lf receptor in the presence of Ca^{2+} ions and GCDCA is K_d = 12.04 μM [128].

2.2. Atom Counting Method

Molecular formulas, empirical formulas, molar masses, and macromolecular composition of Norovirus particles, genomic RNA and VP1 capsid protein were determined, based on genetic and protein sequences and virus morphology, using the atom counting method, as described in [59,130,131]. The atom counting method is a computational method for the calculation of chemical properties of macromolecules and macromolecular assemblies, based on genomic and proteomic data [59,130,132]. The input of the program are genetic sequences, protein sequences and, in case of macromolecular assemblies, morphology [59,130]. Biological macromolecules consist of residues of monomers, like nucleotides and amino acids [59,130]. All the residues have a well-defined elemental composition [59,130]. The program goes along sequences of macromolecules and adds atoms coming from each residue [59,130]. In the case of macromolecular assemblies, the atoms coming from every kind of macromolecule are multiplied by the number of copies of that macromolecule in the particle [59,130]. Adding atoms of all elements in a particle gives its molecular formula [59,130]. To obtain the empirical formula, the numbers of atoms of all constituent elements are divided by the number of carbon atoms [59,130]. Finally, to calculate the macromolecular composition, the molar mass of a macromolecule is multiplied with its number of copies to find the total mass of that macromolecule in the macromolecular assembly. After that, the macromolecules are sorted into types (DNA, RNA, proteins, lipids and carbohydrates) and mass fractions of every type are calculated.

2.3. Patel–Erickson Model

Standard enthalpies of the formation of Norovirus particles, genomic RNA, and VP1 capsid protein were calculated based on empirical formulas with the Patel–Erickson model, as described in [133–135]. The Patel–Erickson model gives enthalpy of live matter based on

its elemental composition [133,134,136,137]. Based on the empirical formula, the degree of reduction, E, is calculated with the equation

$$E = 4n_C + n_H - 2n_O - 0n_N + 5n_P + 6n_S \quad (1)$$

where n_C, n_H, n_O, n_N, n_P, and n_S are numbers of C, H, O, N, P, and S atoms in the empirical formula, respectively [133,134,138]. Then, the degree of reduction is used to find standard enthalpy of combustion, $\Delta_C H^0$, of live matter with the equation [133,134]

$$\Delta_C H^0(bio) = -111.14 \frac{kJ}{C-mol} \cdot E \quad (2)$$

After that, $\Delta_C H^0$ is used to find the standard enthalpy of formation, $\Delta_f H^0$, of live matter, with Hess's law [134,139,140].

$$\Delta_f H^0(bio) = n_C \Delta_f H^0(CO_2) + \frac{n_H}{2} \Delta_f H^0(H_2O) + \frac{n_P}{4} \Delta_f H^0(P_4O_{10}) + n_S \Delta_f H^0(SO_3) - \Delta_C H^0 \quad (3)$$

The Patel–Erickson model is sometimes called Thornton's rule, since it is based on Thornton's theory of combustion [141]. Thornton found that the energy released by combustion comes from acceptance of electrons by oxygen [141]. This is why it is proportional to the number of electrons transferred to oxygen during the process, which is represented by E [133,134].

2.4. Battley Model

Standard molar entropies of Norovirus particles, genomic RNA and VP1 capsid protein were calculated, based on empirical formulas, with the Battley model, as described in [142,143]. The Battley model gives entropy of live matter, based on its elemental composition [142,143]. Standard molar entropy is calculated from the empirical formula with the equation

$$S_m^0(bio) = 0.187 \sum_J \frac{S_m^0(J)}{a_J} n_J \quad (4)$$

where $S^0{}_m(J)$ is standard molar entropy of element J in its standard state elemental (pure) form, a_J number of atoms of element J in its standard state elemental form, and n_J the number of atoms of element J in the empirical formula of live matter [142,143]. Standard entropy of formation, $\Delta_f S^0$, can be found from the following equation [142,143]:

$$\Delta_f S^0(bio) = -0.813 \sum_J \frac{S_m^0(J)}{a_J} n_J \quad (5)$$

The Battley model comes from the additivity property of entropy. Entropy of a complex system is a sum of contributions of its parts. If live matter consists of different elements, then its entropy is proportional to the sum of entropies of the constituent elements (the sum term). The sum term is multiplied by a constant (0.187 or −0.813) to take into account the changed environment of the elements (live matter vs. pure form).

Standard Gibbs energy of formation, $\Delta_f G^0$, of live matter is found from $\Delta_f H^0$ and $\Delta_f S^0$, with the equation

$$\Delta_f G^0(bio) = \Delta_f H^0(bio) - T \Delta_f S^0(bio) \quad (6)$$

where T is temperature [144–146].

2.5. Biosynthesis Reactions

Biosynthesis reactions of Norovirus particles, genomic RNA and VP1 capsid protein were calculated, based on their empirical formulas, with the rules of stoichiometry [147,148].

Biosynthesis reactions are macrochemical equations that explain conversion of nutrients into new live matter in metabolism [53,139,149–152]. The general biosynthesis reaction of viruses has the form [153–155]

$$\text{(Amino acid)} + O_2 + HPO_4^{2-} + HCO_3^- \rightarrow \text{(Bio)} + SO_4^{2-} + H_2O + HCO_3^- + H_2CO_3 \quad (7)$$

The nutrients for biosynthesis of virus live matter include amino acids with the empirical formula $CH_{1.798}O_{0.4831}N_{0.2247}S_{0.022472}$ (source of energy, carbon, nitrogen and sulfur), O_2 (electron acceptor) and HPO_4^{2-} (source of phosphorus) [153–155]. Main products of biosynthesis are new live matter (bio) with the empirical formula $CH_{nH}O_{nO}N_{nN}P_{nP}S_{nS}$, SO_4^{2-} (excess sulfur removal) and H_2CO_3 (oxidized carbon removal) [153–155]. Moreover, the H^+ ions produced during biosynthesis are absorbed by the bicarbonate buffer made of HCO_3^- and H_2CO_3 [153–155].

2.6. Thermodynamic Properties of Biosynthesis

Thermodynamic properties of biosynthesis were calculated with Hess's law [144,145,156,157]. They were calculated by application of Hess's law to biosynthesis reactions and thermodynamic properties of live matter. Thermodynamic properties of biosynthesis include standard enthalpy of biosynthesis, $\Delta_{bs}H^0$, standard entropy of biosynthesis, $\Delta_{bs}S^0$, and standard Gibbs energy of biosynthesis, $\Delta_{bs}G^0$ [53,150,158,159]. They were found with the following equations

$$\Delta_{bs}H^0 = \sum_{products} \nu\Delta_f H^0 - \sum_{reactants} \nu\Delta_f H^0 \quad (8)$$

$$\Delta_{bs}S^0 = \sum_{products} \nu S_m^o - \sum_{reactants} \nu S_m^o \quad (9)$$

$$\Delta_{bs}G^0 = \sum_{products} \nu\Delta_f G^0 - \sum_{reactants} \nu\Delta_f G^0 \quad (10)$$

where $\Delta_f H^0$ is standard enthalpy of formation, ${S_m}^0$ standard molar entropy, $\Delta_f G^0$ standard Gibbs energy of formation and ν represents a stoichiometric coefficient [53,134,139,150,153–155,160].

2.7. Thermodynamic Properties of Binding

The interaction of a virus with its host cell begins at the host cell membrane [161]. There, the virus antigen binds to the host cell receptor [161]. Antigen-receptor binding is a chemical process similar to protein ligand binding [21,162]. Antigen-receptor binding can be represented with the chemical reaction

$$\text{(An)} + \text{(Re)} \rightleftarrows \text{(An-Re)} \quad (11)$$

where (An) is the free virus antigen, (Re) free host receptor and (An-Re) the antigen-receptor complex [21,162]. This reaction can, like all other chemical reactions, be analyzed with the laws of chemical thermodynamics and is characterized with thermodynamic properties. The dissociation equilibrium constant, K_d, is given by the equation

$$K_d = \frac{[An][Re]}{[An - Re]} \quad (12)$$

where [An] is the concentration of the free virus antigen, [Re] the concentration of the free host receptor and [An − Re] the concentration of the antigen-receptor complex [21,162]. K_d for antigen-receptor binding can be measured experimentally with surface plasmon reso-

nance [163] or non-competitive ELISA approach [164]. From K_d, the binding equilibrium constant, K_B, can be determined from the equation [21,162]

$$K_B = \frac{[An - Re]}{[An][Re]} = \frac{1}{K_d} \quad (13)$$

Based on K_B, it is possible to find standard Gibbs energy of binding, $\Delta_B G^0$, with the equation [21,162]

$$\Delta_B G^0 = -RT \ln K_B \quad (14)$$

3. Results

Table 1 presents molecular formulas and molar masses of the Norovirus particle, genomic RNA and VP1 capsid protein. Molecular formulas show the total numbers of atoms of all constituent elements in a molecule or macromolecular assembly (e.g., virus particle). The molecular formulas and molar masses were calculated with the atom counting method, based on genetic and protein sequences and virus morphology, as described in [59,130]. The molecular formula of the Norovirus particle is $C_{548504}H_{817571}O_{193862}N_{157282}P_{7525}S_{3060}$, with a molar mass of 13,048 kDa. The molecular formula of the Norovirus genomic RNA is $C_{71684}H_{88571}O_{52202}N_{28762}P_{7525}$, with a molar mass of 2421.4 kDa. The molecular formula of the Norovirus VP1 capsid protein is $C_{2649}H_{4050}O_{787}N_{714}S_{17}$, with a molar mass of 59.035 kDa.

Table 1. Molecular formulas of the Norovirus particle, genomic RNA and VP1 capsid protein. The molecular formulas have the general form $C_{mC}H_{mH}O_{mO}N_{mN}P_{mP}S_{mS}$, where m_C, m_H, m_O, m_N, m_P and m_S are the numbers of C, H, O, N, P and S atoms in the molecular formula, respectively, which are given in this table. The table also shows molar masses of entire molecules/structures, *Mr* (*tot*).

Name	m_C	m_H	m_O	m_N	m_P	m_S	Mr (kDa)
Norovirus particle	548,504	817,571	193,862	157,282	7525	3060	13,048
Norovirus RNA	71,684	88,571	52,202	28,762	7525	0	2421.4
Norovirus VP1	2649	4050	787	714	0	17	59.035

Table 2 gives the macromolecular composition of the Norovirus particle. The macromolecular composition was calculated with the atom counting method, based on genetic and protein sequences and virus morphology, as described in [59,130] The norovirus particle consists of 18.6% RNA and 81.4% proteins (by mass).

Table 2. Macromolecular composition of the Norovirus particle.

Name	Content (%-Mass)
RNA	18.6
Proteins	81.4

Table 3 shows the empirical formulas of the Norovirus particle, genomic RNA and VP1 capsid protein. Empirical formulas show the numbers of atoms of constituent elements in a molecule or macromolecular assembly (e.g., virus particle) per carbon atom. The empirical formulas and their molar masses were calculated with the atom counting method, based on genetic and protein sequences and virus morphology, as described in [59,130]. The empirical formula of the Norovirus particle is $CH_{1.4905}O_{0.3534}N_{0.2867}P_{0.013719}S_{0.005579}$, with a molar mass of 23.79 g/C-mol. The empirical formula of the Norovirus genomic RNA is $CH_{1.2356}O_{0.7282}N_{0.4012}P_{0.104975}$, with a molar mass of 33.78 g/C-mol. The empirical formula

of the Norovirus VP1 capsid protein is $CH_{1.5289}O_{0.2971}N_{0.2695}S_{0.006418}$, with a molar mass of 22.29 g/C-mol.

Table 3. Empirical formulas of the Norovirus particle, genomic RNA, and VP1 capsid protein. Empirical formulas show the number of atoms of each element present per carbon atom. The empirical formulas have the general form $CH_{nH}O_{nO}N_{nN}P_{nP}S_{nS}$, where n_H, n_O, n_N, n_P and n_S are the numbers of H, O, N, P and S atoms in the empirical formula, respectively, which are given in this table. The table also gives molar masses of empirical formulas, *Mr*.

Name	n_H	n_O	n_N	n_P	n_S	Mr (g/C-mol)
Norovirus particle	1.4905	0.3534	0.2867	0.013719	0.005579	23.79
Norovirus RNA	1.2356	0.7282	0.4012	0.104975	0.000000	33.78
Norovirus VP1	1.5289	0.2971	0.2695	0.000000	0.006418	22.29

Table 4 gives thermodynamic properties of live matter of Norovirus particles, genomic RNA and VP1 capsid protein. These include standard enthalpy of formation, $\Delta_f H^0$, standard molar entropy, ${S_m}^0$, and standard Gibbs energy of formation, $\Delta_f G^0$. They were calculated with the Patel–Erickson model [133,134] and Battley model [142,143], based on the empirical formulas from Table 3. Like the empirical formulas, the thermodynamic properties of live matter ($\Delta_f H^0$, ${S_m}^0$ and $\Delta_f G^0$) are inherent properties of live matter and do not depend on the way that live matter produced by organisms (biosynthesis reactions). For the Norovirus particle, standard enthalpy of formation is −76.06 kJ/C-mol, standard molar entropy is 31.30 kJ/C-mol and standard Gibbs energy of formation is −35.49 kJ/C-mol. For the Norovirus genomic RNA, standard enthalpy of formation is −170.69 kJ/C-mol, standard molar entropy is 38.09 kJ/C-mol and standard Gibbs energy of formation is −121.32 kJ/C-mol. For the Norovirus VP1 capsid protein, standard enthalpy of formation is −61.83 kJ/C-mol, standard molar entropy is 30.28 kJ/C-mol and standard Gibbs energy of formation is −22.58 kJ/C-mol.

Table 4. Thermodynamic properties of Norovirus particles, genomic RNA, and VP1 capsid protein: standard enthalpy of formation, $\Delta_f H^0$, standard molar entropy, ${S_m}^0$, and standard Gibbs energy of formation, $\Delta_f G^0$.

Name	$\Delta_f H^0$ (kJ/C-mol)	${S_m}^0$ (J/C-mol K)	$\Delta_f G^0$ (kJ/C-mol)
Norovirus particle	−76.06	31.30	−35.49
Norovirus RNA	−170.69	38.09	−121.32
Norovirus VP1	−61.83	30.28	−22.58

Table 5 presents stoichiometric coefficients for the biosynthesis reactions of the Norovirus particles, genomic RNA and VP1 capsid protein. They were calculated with stoichiometry, based on the empirical formulas from Table 3. Biosynthesis reactions show how new live matter is produced by organisms from nutrients. The biosynthesis reaction of the Norovirus has the general form (Amino acid) + O_2 + HPO_4^{2-} + HCO_3^- → (Bio) + SO_2^{2-} + H_2O + HCO_3^- + H_2CO_3, where (Amino acid) represents amino acids with the empirical formula $CH_{1.798}O_{0.4831}N_{0.2247}S_{0.022472}$ and (Bio) represents the empirical formula of live matter.

Table 5. Biosynthesis stoichiometries of Norovirus particles, genomic RNA and VP1 capsid protein. The general biosynthesis reaction has the following form: (Amino acid) + O_2 + HPO_4^{2-} + HCO_3^- → (Bio) + SO_2^{2-} + H_2O + HCO_3^- + H_2CO_3. "Amino acid" represents amino acids with the empirical formula $CH_{1.798}O_{0.4831}N_{0.2247}S_{0.022472}$. "Bio" represents the empirical formula of live matter from Table 1.

Name	Reactants				→	Products				
	Amino acid	O_2	HPO_4^{2-}	HCO_3^-		Bio	SO_4^{2-}	H_2O	HCO_3^-	H_2CO_3
Norovirus particle	1.2760	0.3628	0.0137	0.0188	→	1	0.0231	0.1232	0.0000	0.2948
Norovirus RNA	1.7855	1.1408	0.1050	0.0000	→	1	0.0401	0.3190	0.1297	0.6558
Norovirus VP1	1.1994	0.2459	0.0000	0.0411	→	1	0.0205	0.0937	0.0000	0.2405

Table 6 gives thermodynamic properties of biosynthesis of Norovirus particles, genomic RNA and VP1 capsid protein. They were calculated with Hess's law [144,145], based on the biosynthesis reactions (from Table 5) and empirical formulas (from Table 3). Thermodynamic properties of biosynthesis are changes in thermodynamic properties during biosynthesis reactions. They are thermodynamic properties of the biosynthesis process and show how thermodynamic properties change during biosynthesis in organisms. They include standard enthalpy of biosynthesis, $\Delta_{bs}H^0$, standard entropy of biosynthesis, $\Delta_{bs}S^0$, and standard Gibbs energy of biosynthesis, $\Delta_{bs}G^0$. For the Norovirus particle, standard enthalpy of biosynthesis is −170.79 kJ/C-mol, standard entropy of biosynthesis −27.12 J/C-mol K and standard Gibbs energy of biosynthesis is −162.85 kJ/C-mol. For the Norovirus genomic RNA, standard enthalpy of biosynthesis is −519.57 kJ/C-mol, standard entropy of biosynthesis −104.02 J/C-mol K and standard Gibbs energy of biosynthesis is −489.79 kJ/C-mol. For the Norovirus VP1 capsid protein, standard enthalpy of biosynthesis is −118.35 kJ/C-mol, standard entropy of biosynthesis −15.56 J/C-mol K and standard Gibbs energy of biosynthesis is −113.70 kJ/C-mol.

Table 6. Thermodynamic properties of biosynthesis of Norovirus particles, genomic RNA and VP1 capsid protein: standard enthalpy of biosynthesis, $\Delta_{bs}H^0$, standard entropy of biosynthesis, $\Delta_{bs}S^0$, and standard Gibbs energy of biosynthesis, $\Delta_{bs}G^0$. Thermodynamic properties of biosynthesis are changes in thermodynamic properties brought about by biosynthesis reactions.

Name	$\Delta_{bs}H^0$ (kJ/C-mol)	$\Delta_{bs}S^0$ (J/C-mol K)	$\Delta_{bs}G^0$ (kJ/C-mol)
Norovirus particle	−170.79	−27.12	−162.85
Norovirus RNA	−519.57	−104.02	−489.79
Norovirus VP1	−118.35	−15.56	−113.70

Table 7 shows thermodynamic properties of antigen-receptor binding of the Norovirus. They were calculated with chemical thermodynamics [144,145], based on literature K_d values [128,129]. Thermodynamic properties of binding are changes in thermodynamic properties during the process of binding of the virus antigen to the host cell receptor. For binding of the Norovirus VP1 protruding domain to the CD300lf receptor alone (in the absence of Ca^{2+}, Mg^{2+} and GCDCA), the binding equilibrium constant is 4.57×10^3 M^{-1} and standard Gibbs energy of binding is −20.89 kJ/mol. For binding of the Norovirus VP1 protruding domain to the CD300lf receptor in the presence of Ca^{2+} ions, the binding equilibrium constant is 4.08×10^4 M^{-1} and standard Gibbs energy of binding is −26.32 kJ/mol. For binding of the Norovirus VP1 protruding domain to the CD300lf receptor in the presence of Mg^{2+} and EGTA, the binding equilibrium constant is 4.12×10^4 M^{-1} and standard Gibbs energy of binding is −26.34 kJ/mol. For binding of the Norovirus VP1 protruding do-

main to the CD300lf receptor in the presence of Ca^{2+} and GCDCA, the binding equilibrium constant is 8.31×10^4 M^{-1} and standard Gibbs energy of binding is −28.08 kJ/mol.

Table 7. Thermodynamic properties of antigen-receptor binding of Murine norovirus (MNoV): dissociation equilibrium constant, K_d; binding equilibrium constant, K_B; and standard Gibbs energy of binding, $\Delta_B G^0$. EGTA denotes ethylene glycol-bis(β-aminoethyl ether)-*N*,*N*,*N*′,*N*′-tetraacetic acid, while GCDCA denotes glycochenodeoxycholic acid. The K_d values were taken from [128,129].

Interaction	Conditions	K_d (M)	K_B (M^{-1})	$\Delta_B G^0$ (kJ/mol)
VP1 protruding (P) domain with CD300lf receptor	Alone	2.19×10^{-4}	4.57×10^3	−20.89
	Ca^{2+}	2.45×10^{-5}	4.08×10^4	−26.32
	Mg^{2+} and EGTA	2.43×10^{-5}	4.12×10^4	−26.34
	Ca^{2+} and GCDCA	1.20×10^{-5}	8.31×10^4	−28.08

4. Discussion

Norovirus is a major cause of viral gastroenteritis worldwide [1,2] and represents an emerging pathogen that poses a risk for human health [3]. Norovirus, like other viruses, lacks cellular metabolic machinery and performs its lifecycle in host cells [165–168]. Viruses hijack their host cell metabolic machinery to perform their own metabolic processes and multiply [169–172]. Virus–host interactions are processes performed by organisms, which are greatly dependent on energetic constraints and can therefore be analyzed with the methodology of biothermodynamics [15,22,70,173,174].

Organisms represent open thermodynamic systems with the property of growth [53,154,175,176]. These systems consist of live matter, which is separated from the environment [177–179]. They perform biological processes, like metabolism and multiplication [60]. To analyze biological processes from the perspective of biothermodynamics, it is necessary to find empirical formulas and thermodynamic properties of live matter [180–182]. Therefore, the biothermodynamic analysis of the Norovirus lifecycle begins with determination of its molecular formula, empirical formula and thermodynamic properties of live matter. Based on these, a model of multiplication of Norovirus inside its host cells will be developed, based on biosynthesis reactions and thermodynamic properties of biosynthesis. Moreover, thermodynamic properties of antigen-receptor binding will be determined. The thermodynamic properties of binding and biosynthesis will be used to analyze the interaction of the Norovirus with its host cells, as well as with the Rotavirus, based on nonequilibrium thermodynamics.

4.1. Chemical and Thermodynamic Properties of the Norovirus

The molecular formula of the Norovirus particle is $C_{548504}H_{817571}O_{193862}N_{157282}P_{7525}S_{3060}$ (Table 1). The molecular formulas of the constituents of the Norovirus particle are: $C_{71684}H_{88571}O_{52202}N_{28762}P_{7525}$ for the genomic RNA and $C_{2649}H_{4050}O_{787}N_{714}S_{17}$ for the VP1 capsid protein (Table 1). The molar mass of the entire norovirus particle is 13 MDa. The molar mass of the VP1 capsid protein was found to be 59 kDa (Table 1). This is in good agreement with the experimental value of 58–60 kDa [183,184].

Molecular formulas of other viruses have been reported in the literature. The molecular formula of the Poliovirus particle is $C_{332652}H_{492388}N_{98245}O_{131196}P_{7501}S_{2340}$ [42,185]. The Poliovirus particle has a diameter of 25 to 30 nm [186]. The molecular formula of the Rotavirus particle is $C_{4589530}H_{7046535}O_{1530010}N_{1249723}P_{37124}S_{34560}$ [14], which has a molar mass of 106.47 MDa [14] and diameter of 70 nm [187]. The molecular formula of the West Nile virus is $C_{1.54 \times 10^6}H_{2.71 \times 10^6}O_{4.01 \times 10^5}N_{2.26 \times 10^5}P_{3.03 \times 10^4}S_{5.76 \times 10^3}$ [154], which has a molar mass of 31.91 MDa [154] and a diameter of 50 nm [188]. The molecular formula of the virus particle of the JN.1 variant of SARS-CoV-2 is $C_{1.01 \times 10^7}H_{1.66 \times 10^7}O_{2.87 \times 10^6}N_{2.32 \times 10^6}P_{6.51 \times 10^4}S_{3.80 \times 10^4}$ [24],

which has a molar mass of 219.7 MDa [24] and a diameter of 60–140 nm [189]. On the other hand, the molecular formula of the Norovirus particle is $C_{548504}H_{817571}O_{193862}N_{157282}P_{7525}S_{3060}$, with a molar mass of 13 MDa (Table 1). Its diameter is 27 nm [190]. Therefore, it can be seen that every virus has a characteristic molecular formula. This means that the molecular and empirical formulas can be used for rapid identification of viruses, especially for emerging viruses when little information is available about their properties. This is in agreement with the result that single-particle ICP-MS can be used for identification of viruses [191].

Based on the molecular formulas, empirical formulas of the norovirus particle, RNA and VP1 capsid protein were calculated for the first time in this research and are shown in Table 3. Empirical formulas are important since they can be used to analyze multiplication of viruses through biosynthesis reactions, as will be discussed below. The empirical formula of the Norovirus particle is $CH_{1.4905}O_{0.3534}N_{0.2867}P_{0.013719}S_{0.005579}$ (Table 3). The empirical formula of the constituents of the Norovirus particle are $CH_{1.2356}O_{0.7282}N_{0.4012}P_{0.104975}$ for the genomic RNA and $CH_{1.5289}O_{0.2971}N_{0.2695}S_{0.006418}$ for the VP1 capsid protein (Table 3). The empirical formula of the Norovirus particle resembles more closely that of the VP1 capsid protein in the content of H, O and S. The reason for this is that the protein is present in a greater amount in the virus particle than the RNA (Table 2). However, the virus particle also contains P, which is absent in proteins, but is present in the RNA.

Empirical formulas have been reported in the literature for other microorganisms. The empirical formula of the nucleocapsid of XBB.1.5 Kraken variant of SARS-CoV-2 is $CH_{1.573540}O_{0.342703}N_{0.312374}P_{0.00603}S_{0.00336}$ [153]. The empirical formula of the bacterium *Escherichia coli* is $CH_{1.918}O_{0.528}N_{0.257}P_{1.76\times10^{-2}}S_{5.54\times10^{-3}}K_{5.87\times10^{-3}}Mg_{2.07\times10^{-3}}Ca_{8.36\times10^{-4}}Mn_{9.89\times10^{-6}}Fe_{7.82\times10^{-5}}Cu_{1.62\times10^{-6}}Zn_{2.41\times10^{-5}}$ [192]. The empirical formula of the yeast *Saccharomyces cerevisiae* is $CH_{1.613}O_{0.557}N_{0.158}P_{0.012}S_{0.003}K_{0.022}Mg_{0.003}Ca_{0.001}$ [134]. The empirical formula of the filamentous fungus *Penicillium chrysogenum* is $CH_{2.026}O_{0.511}N_{0.185}P_{9.15\times10^{-3}}S_{4.17\times10^{-3}}K_{3.45\times10^{-3}}Mg_{1.47\times10^{-3}}Ca_{3.69\times10^{-4}}Mn_{1.08\times10^{-5}}Fe_{9.51\times10^{-5}}Cu_{1.24\times10^{-6}}Zn_{2.15\times10^{-5}}$ [192]. Therefore, every microorganism species has a characteristic empirical formula different from those of other microorganisms.

Based on the empirical formulas, thermodynamic properties of live matter were determined for the first time for Norovirus particles, genomic RNA and VP1 capsid protein, which are shown in Table 4. The Norovirus particle is characterized with a standard Gibbs energy of formation of −35.49 kJ/C-mol. Gibbs energies of the formation of Norovirus particle components are −121.32 kJ/C-mol for the genomic RNA and −22.58 kJ/C-mol for the VP1 capsid protein. Gibbs energy of formation of the VP1 capsid protein is greater (less negative) than that of the genomic RNA. This means that the VP1 capsid protein has a greater usable energy content than that of the genomic RNA.

Every virus species has a specific genetic and protein sequences. This us why it has an empirical formula different from other viruses. The different empirical formulas lead to different thermodynamic properties of live matter. Empirical formulas and thermodynamic properties of live matter are used to formulate biosynthesis reactions and calculate thermodynamic properties of biosynthesis, which show the energetic requirements and rates of virus multiplication. This means that biothermodynamic methodology has a potential to show how different genetic and protein sequences viruses can lead to different rates of multiplication and pathogenicity.

4.2. Virus–Host Interactions of the Norovirus with Enterocytes

Based on the determined empirical formulas and thermodynamic properties of the Norovirus, a biothermodynamic model of the interactions of Norovirus with its host cells will be developed. This will be carried out with biosynthesis equations, thermodynamic properties of biosynthesis and phenomenological equations.

Biosynthesis reactions are macrochemical reactions that show how nutrients are transformed into new live matter by organisms [150,193]. The biosynthesis reaction of the Norovirus particles is

$$1.2760\ CH_{1.798}O_{0.4831}N_{0.2247}S_{0.022472} + 0.3628\ O_2 + 0.0137\ HPO_4^{2-} + 0.0188\ HCO_3^- \rightarrow CH_{1.4905}O_{0.3534}N_{0.2867}P_{0.013719}S_{0.005579} + 0.0231\ SO_2^{2-} + 0.1232\ H_2O + 0.2948\ H_2CO_3 \quad (15)$$

where $CH_{1.798}O_{0.4831}N_{0.2247}S_{0.022472}$ represents amino acids and $CH_{1.4905}O_{0.3534}N_{0.2867}P_{0.013719}S_{0.005579}$ is the empirical formula of newly synthetized Norovirus particles (Table 5).

Biosynthesis reactions were also found for the constituents of the Norovirus particles: RNA and VP1 capsid proteins. The biosynthesis reaction of the genomic RNA of the Norovirus is

$$1.7855\ CH_{1.798}O_{0.4831}N_{0.2247}S_{0.022472} + 1.1408\ O_2 + 0.1050\ HPO_4^{2-} \rightarrow CH_{1.2356}O_{0.7282}N_{0.4012}P_{0.104975} + 0.0401\ SO_2^{2-} + 0.3190\ H_2O + 0.1297\ HCO_3^- + 0.6558\ H_2CO_3 \quad (16)$$

where $CH_{1.2356}O_{0.7282}N_{0.4012}P_{0.104975}$ is the empirical formula of Norovirus genomic RNA (Table 5). The biosynthesis reaction of the Norovirus VP1 capsid protein is

$$1.1994\ CH_{1.798}O_{0.4831}N_{0.2247}S_{0.022472} + 0.2459\ O_2 + 0.0411\ HCO_3^- \rightarrow CH_{1.5289}O_{0.2971}N_{0.2695}S_{0.006418} + 0.0205\ SO_2^{2-} + 0.0937\ H_2O + 0.2405\ H_2CO_3 \quad (17)$$

where $CH_{1.5289}O_{0.2971}N_{0.2695}S_{0.006418}$ is the empirical formula of the Norovirus VP1 capsid protein (Table 5). The biosynthesis reaction of the Norovirus particle is more similar to that of the VP1 capsid protein than that of the genomic RNA, in the stoichiometric coefficients for amino acids, O_2 and SO_2^{2-}. The reason for this is that the VP1 capsid proteins comprise a larger portion of the Norovirus particle. This means that biosynthesis of the VP1 protein takes a major part of the nutrients required to produce the Norovirus particle. However, the biosynthesis reaction of the Norovirus particle also contains HPO_4^{2-}, which is not present in the biosynthesis reaction of the VP1 capsid protein, but is needed to produce the genomic RNA.

Biosynthesis reactions lead to change in Gibbs energy, which is called Gibbs energy of biosynthesis [53,150]. Gibbs energy of biosynthesis of the Norovirus is −162.85 kJ/C-mol (Table 6). Norovirus replicates in the intestinal tissue [194]. The biosynthesis reaction of the small intestine tissue is

$$0.7961\ CH_{1.798}O_{0.4831}N_{0.2247}S_{0.022472} + 0.3211\ CH_2O + 0.0028\ HPO_4^{2-} + 0.0252\ HCO_3^- + 0.0038\ Na^+ + 0.0044\ K^+ + 0.0024\ Cl^- \rightarrow CH_{1.6480}O_{0.2310}N_{0.1789}P_{0.0028}S_{0.0054}Na_{0.0038}K_{0.0044}Cl_{0.0024} + 0.0125\ SO_2^{2-} + 0.0843\ H_2O + 0.1423\ H_2CO_3 \quad (18)$$

where CH_2O is the empirical formula of carbohydrates and $CH_{1.6480}O_{0.2310}N_{0.1789}P_{0.0028}S_{0.0054}Na_{0.0038}K_{0.0044}Cl_{0.0024}$ is the empirical formula of live matter of the small intestine tissue [43]. Gibbs energy of biosynthesis of the small intestine tissue is −16.85 kJ/C-mol [43]. Thus, the Gibbs energy of the biosynthesis of the Norovirus is much more negative than that of its host tissue.

The biosyntheses of new virus particles and host cell building blocks are chemical reactions that are out of equilibrium [17,53,54]. These reactions (Equations (15) and (18)) share the same reactants, like amino acids. This means that new virus particles and host cell building blocks are produced from the same precursors [43,195,196]. A precursor molecule can either be incorporated into a new virus particle or a host cell structure. Since the amount of precursors is limited, the virus and its host cell must compete [8,197,198]. Therefore, the biosynthesis of new virus particles and host cell building blocks are competitive chemical reactions.

Since virus multiplication and biosynthesis of host cell building blocks are nonequilibrium processes, they can be analyzed with the methodology of nonequilibrium thermo-

dynamics [54,70,199]. Phenomenological equations belong to nonequilibrium thermodynamics and show how rates of processes depend on their driving forces [54,177]. Gibbs energy of biosynthesis represents the driving force of the biosynthesis process [54,155,200]. The biosynthesis phenomenological equation shows how biosynthesis rate, r_{bs}, depends on Gibbs energy of biosynthesis, $\Delta_{bs}G$:

$$r_{bs} = -\frac{L_{bs}}{T}\Delta_{bs}G \tag{19}$$

where L_{bs} is the biosynthesis phenomenological coefficient [154,179,201]. Due to the minus sign, a more negative Gibbs energy of biosynthesis implies a greater biosynthesis rate.

Gibbs energy of biosynthesis of the Norovirus is −162.85 kJ/C-mol (Table 6), while that of the small intestine tissue is −16.85 kJ/C-mol [43]. Thus, the Norovirus has a much more negative Gibbs energy of biosynthesis than its host tissue. This means that, according to the biosynthesis phenomenological equation, it can achieve a much greater biosynthesis rate. Due to the greater rate of the Norovirus biosynthesis reaction, more precursors will be consumed by the biosynthesis of new virus particles. Additionally, the host cell metabolic machinery will produce more virus particles than host cell building blocks. In that way, the virus will hijack the host cell metabolic machinery for its multiplication.

Due to the more negative Gibbs energy of biosynthesis, the virus will have a higher biosynthesis rate. Due to the higher biosynthesis rate, more resources will be consumed by the production of new virus particles and the host cell metabolic machinery will produce more new virus particles than host cell building blocks. Since the host cell metabolic machinery produces mostly new virus particles, it is hijacked by the virus.

Except for biosynthesis precursors, viruses also compete with their host cells for metabolic energy, which comes in the form of ATP [202,203]. Viral multiplication and host cell metabolic processes use the common stock of cellular ATP. Therefore, the virus has to compete with its host cell for ATP. Fast replicating viruses may even hijack and compartmentalize the energy-producing enzymes to provide a readily available source of ATP for viral replication [202]. Moreover, some viruses hijack cellular metabolic enzymes to reprogram cell metabolism and stimulate ATP production in processes like glycolysis [203]. However, ATP itself is not the ultimate source of energy in a cell. Energy comes from degradation of nutrients in catabolic processes [53,134,150]. ATP just transfers energy from catabolic to anabolic processes [53,150,204]. The generation of more ATP causes the upregulation of catabolism. Faster catabolism is needed to generate more ATP, which is needed for virus replication. However, the virus and its host cell share the cellular metabolic machinery. This means that increase in catabolism rate generates more ATP, which can be used not only by the virus, but also by the host cell. A higher catabolism rate and more ATP provide a greater potential for biosynthesis processes. However, this potential still has to be exploited by the virus. If a virus has a Gibbs energy of biosynthesis equal to that of the host cell, then the excess ATP can be used equally to drive the biosynthesis of new viruses and host cell building blocks. In order to exploit the excess ATP, the virus must have a greater biosynthesis rate. A greater biosynthesis rate implies that the biosynthesis of new virus particles will proceed at a greater rate than that of host cell building blocks. Due to the greater reaction rate, the rate of consumption of ATP by the virus will be greater than that of its host cell. In this way, the virus will be able to exploit the increase in ATP production by catabolism.

In order to perform its lifecycle inside a host cell, a virus must enter the host cell [161]. The virus achieves this through the process of antigen-receptor binding [18,19]. Antigen-receptor binding represents a chemical process [10,15,22]. The driving force of antigen-receptor binding is Gibbs energy of binding [21]. The rate of antigen-receptor binding,

r_B, depends on Gibbs energy of binding, $\Delta_B G$, according to the binding phenomenological equation

$$r_B = -\frac{L_B}{T}\Delta_B G \quad (20)$$

where L_B is the binding phenomenological coefficient [21]. A virus with a more negative Gibbs energy of binding will achieve a greater binding rate [21,153,173]. This will allow it to enter its host cells more efficiently [21,153,173]. Gibbs energy of binding of the Norovirus is between −20.89 and −28.08 kJ/mol (Table 7). The negative Gibbs energy of binding means that the antigen-receptor binding is a spontaneous process, and the virus will be able to infect a host cell that possesses the appropriate receptor.

Susceptibility and permissiveness are important properties of interactions between viruses and their host cells. Susceptibility shows the ability of a virus to enter into its host cell [205–207]. Permissiveness represents the potential of a virus to multiply inside the host cell [205,206]. To achieve a successful infection, a virus must enter a cell that is susceptible and permissive [205,206]. Susceptibility and permissiveness can be analyzed with the methodology of biothermodynamics. Gibbs energy of binding shows the ability of viruses to enter into host cells. A virus must have a negative Gibbs energy of binding to enter into a host cell. A more negative Gibbs energy of binding implies a greater rate of binding and entry into host cells, according to the binding phenomenological equation. This means that Gibbs energy of binding indicates susceptibility. Additionally, Gibbs energy of biosynthesis shows the ability of a virus to multiply inside a host cell. A virus must have a more negative Gibbs energy of binding than its host cell to multiply, according to the biosynthesis phenomenological equation. This means that Gibbs energy of biosynthesis indicates permissiveness. Therefore, biothermodynamics can be used to determine susceptibility and permissiveness of viruses, based on their genetic sequences, protein sequences and morphologies. This means that biothermodynamics can show susceptibility and permissiveness of cells to viruses when little information about them is available. This means that biothermodynamics methodology can be a useful tool for analysis of emerging viruses.

4.3. Virus–Virus Interaction of Norovirus with Rotavirus

Noroviruses and Rotaviruses are among leading causes of acute gastroenteritis worldwide [208–210]. The host cells of the Norovirus and Rotavirus are enterocytes [194,211]. Therefore, it is interesting to analyze what happens when the Norovirus and Rotavirus circulate in a population, at the same time. Gibbs energy of binding of the Rotavirus is between −24.69 and −22.20 kJ/mol [14]. The biosynthesis reaction of the Rotavirus is

$$\begin{aligned} 1.2117\ CH_{1.798}O_{0.4831}N_{0.2247}S_{0.022472} + 0.2659\ O_2 + 0.0081\ HPO_4{}^{2-} + 0.0232\ HCO_{3-} \rightarrow \\ CH_{1.5354}O_{0.3334}N_{0.2723}P_{0.008089}S_{0.007530} + 0.0197\ SO_2{}^{2-} + 0.1022\ H_2O + 0.2350\ H_2CO_3 \end{aligned} \quad (21)$$

where $CH_{1.5354}O_{0.3334}N_{0.2723}P_{0.008089}S_{0.007530}$ is the empirical formula of newly formed virus particles [14]. Gibbs energy of biosynthesis of the Rotavirus is −120.95 kJ/C-mol [14]. On the other hand, Norovirus is characterized by a Gibbs energy of binding between −20.89 and −28.08 kJ/mol (Table 7) and Gibbs energy of biosynthesis of −162.85 kJ/C-mol (Table 6). Therefore, Norovirus and Rotavirus have similar Gibbs energies of binding (Figure 1). This means that Norovirus and Rotavirus will enter into host cells at similar rates. However, Gibbs energy of biosynthesis of Norovirus is more negative than that of Rotavirus (Figure 2). This means that Norovirus will multiply faster in host cells. This means that if Norovirus and Rotavirus circulate in the population at the same time, Norovirus will have an advantage over Rotavirus in multiplication inside host cells, while both viruses will enter into host cells at the same rate. This means that the Norovirus should have a slight advantage over Rotavirus. However, this is not enough for Norovirus

to suppress Rotavirus, and both viruses will be present in the population. Thus, Norovirus and Rotavirus should be able to perform coinfection. Indeed, Norovirus and Rotavirus have been reported in the literature to perform coinfection [212–219].

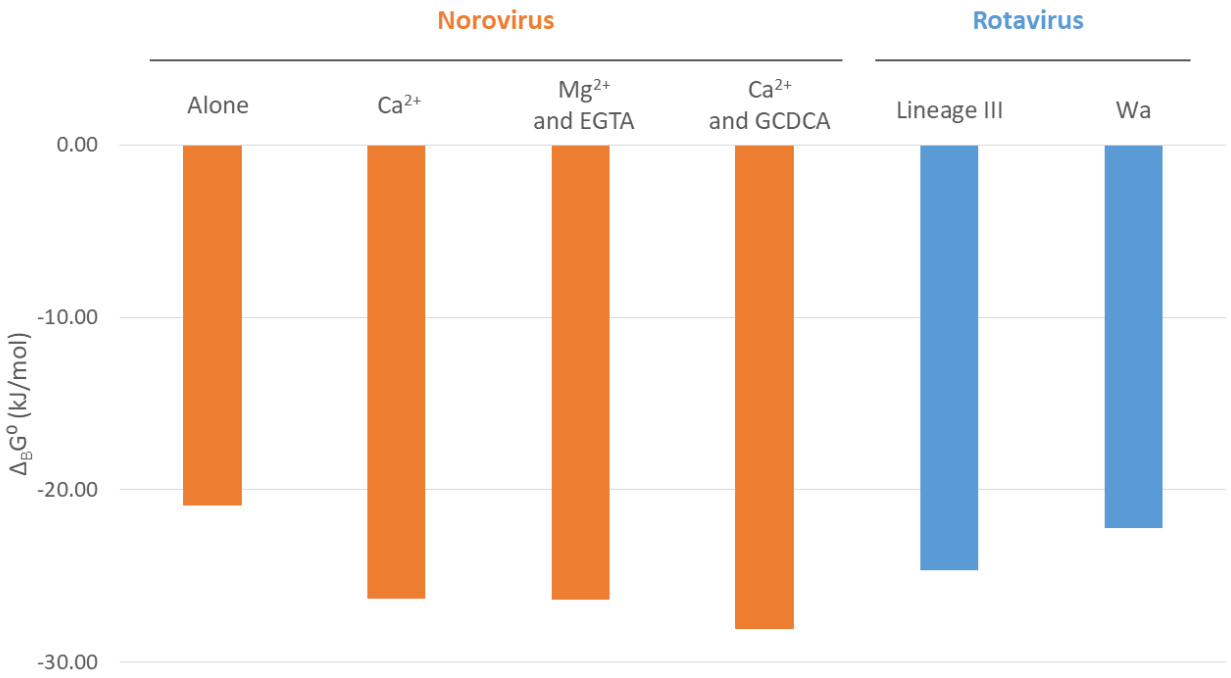


Figure 1. Standard Gibbs energies of binding, $\Delta_B G^0$, of Norovirus and Rotavirus to host cell receptors.

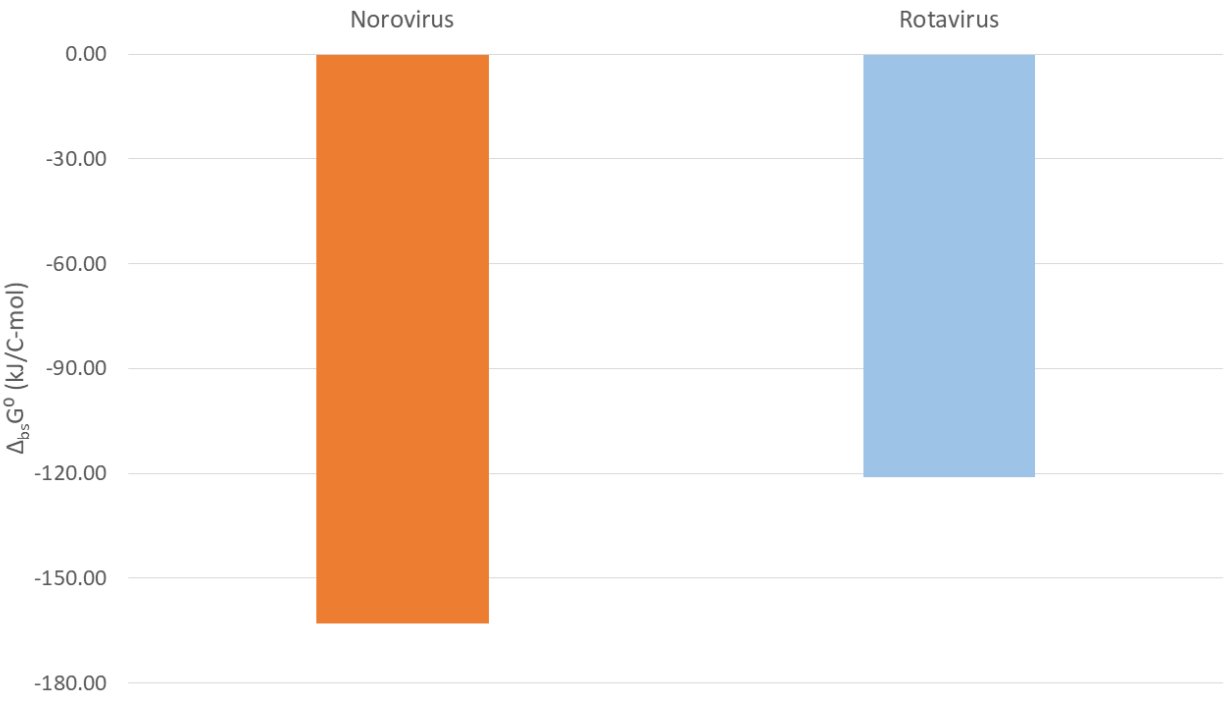


Figure 2. Standard Gibbs energies of biosynthesis, $\Delta_{bs} G^0$, of Norovirus and Rotavirus.

5. Conclusions

The empirical formula and thermodynamic properties of Norovirus were determined for the first time. The empirical formula of the Norovirus particle is $CH_{1.4905}O_{0.3534}N_{0.2867}P_{0.013719}S_{0.005579}$. The empirical formula of the Norovirus genomic RNA is $CH_{1.2356}O_{0.7282}N_{0.4012}P_{0.104975}$, while that of the VP1 capsid protein is $CH_{1.5289}O_{0.2971}N_{0.2695}S_{0.006418}$. Gibbs

energy of formation of the Norovirus particle is −35.49 kJ/C-mol. The empirical formula and Gibbs energy of formation of Norovirus are different from those of other microorganisms. Norovirus has a Gibbs energy of binding between −20.89 and −28.08 kJ/mol.

A biothermodynamic analysis of the interactions of Norovirus with its host cells was conducted. Gibbs energy of biosynthesis of the Norovirus is −162.85 kJ/C-mol. On the other hand, Gibbs energy of biosynthesis of enterocytes is −16.85 kJ/C-mol. Therefore, the virus has a much more negative Gibbs energy of biosynthesis than its host cell. New virus particles and host cell building blocks are produced from the same precursors, like amino acids. A precursor molecule can either be incorporated into a new virus particle or a structure of the host cell. This is why the virus and host cell compete for precursors. Virus multiplication and biosynthesis of host cell building blocks are processes out of equilibrium. This means that they are governed by phenomenological equations of nonequilibrium thermodynamics. According to phenomenological equations, the rate of biosynthesis will be higher for a process with more negative Gibbs energy. Therefore, since the virus has a more negative Gibbs energy, biosynthesis of new virus particles will be faster than biosynthesis of the host cell building blocks. Due to the greater biosynthesis rate, more precursors will be consumed by the biosynthesis of new virus particles. Additionally, the host cell metabolic machinery will produce much more virus particles than host cell building blocks. In that way, the virus will hijack the host cell metabolic machinery for its multiplication. Therefore, due to the more negative Gibbs energy of biosynthesis, the virus will have a higher biosynthesis rate. Due to the higher biosynthesis rate, resources will be diverted into production of new virus particles and the host cell metabolic machinery will produce new virus particles more than host cell building blocks. Since the host cell metabolic machinery produces mostly new virus particles, it is hijacked by the virus.

Except for biosynthesis precursors, the virus and its host cell compete for metabolic energy, which comes in the form of a shared cellular stock of ATP. ATP transfers energy from catabolism where it is generated to biosynthesis processes. Some viruses upregulate catabolism to produce more ATP, which can be used for the production of new virus particles. However, the increased production of ATP provides a higher potential for biosynthesis not only for the virus, but also for its host cell. In order to exploit the increased ATP production, the virus must have a higher biosynthesis rate than its host cell. Due to the higher biosynthesis rate, production of new viruses will consume more ATP than production of host cell building blocks. To achieve a higher biosynthesis rate, the virus must have a more negative Gibbs energy of biosynthesis than its host cell. Therefore, the more negative Gibbs energy allows the virus to exploit the increased potential for biosynthesis provided by upregulated catabolism and increased ATP production.

An analysis was made of the virus–virus interactions between Norovirus and Rotavirus. Norovirus and Rotavirus have similar Gibbs energies of binding. This means that both viruses will be able to enter into host cells at similar rates. Norovirus has a more negative Gibbs energy of biosynthesis than Rotavirus, which means that it should multiply faster in host cells. This gives Norovirus an advantage, but is not enough to allow it to suppress Rotavirus. Therefore, Norovirus and Rotavirus should be able to perform coinfection.

Author Contributions: M.E.P.: Conceptualization; Methodology; Software; Validation; Formal analysis; Investigation; Data Curation; Writing—Original Draft; Writing—Review and Editing; Visualization; V.T.: Validation; Resources; Writing—Review and Editing; Funding acquisition; M.P.P.: Validation; Resources; Writing—Review and Editing; Funding acquisition. All authors have read and agreed to the published version of the manuscript.

Funding: This research was funded by the Ministry of Science, Technological Development and Innovation of the Republic of Serbia grant number 451-03-136/2025-03/200026.

Institutional Review Board Statement: Not applicable.

Informed Consent Statement: Not applicable.

Data Availability Statement: The data presented in this study are available on request from the corresponding author.

Conflicts of Interest: The authors declare no conflict of interest.

References

1. Saito, H.; Toho, M.; Tanaka, T.; Noda, M. Chapter 10—"PANtrap": A Novel Detection Method for General Food Samples. In *The Norovirus*; Chan, P.K.S., Ed.; Academic Press: Amsterdam, The Netherlands, 2017; pp. 145–153. [CrossRef]
2. Ahmed, S.M.; Hall, A.J.; Robinson, A.E.; Verhoef, L.; Premkumar, P.; Parashar, U.D.; Koopmans, M.; Lopman, B.A. Global prevalence of norovirus in cases of gastroenteritis: A systematic review and meta-analysis. *Lancet Infect. Dis.* **2014**, *14*, 725–730. [CrossRef] [PubMed]
3. Lu, M.C.; Lin, S.C.; Hsu, Y.H.; Chen, S.Y. Epidemiology, Clinical Features, and Unusual Complications of Norovirus Infection in Taiwan: What We Know after Rotavirus Vaccines. *Pathogens* **2022**, *11*, 451. [CrossRef] [PubMed]
4. Popović, M.E.; Tadić, V.; Popović, M. (R)evolution of Viruses: Introduction to biothermodynamics of viruses. *Virology* **2025**, *603*, 110319. [CrossRef] [PubMed]
5. Lucia, U.; Grisolia, G.; Deisboeck, T.S. Thermodynamics and SARS-CoV-2: Neurological effects in post-Covid 19 syndrome. *Atti Della Accad. Peloritana Pericolanti* **2021**, *99*, A3. [CrossRef]
6. Kaniadakis, G.; Baldi, M.M.; Deisboeck, T.S.; Grisolia, G.; Hristopulos, D.T.; Scarfone, A.M.; Sparavigna, A.; Wada, T.; Lucia, U. The κ-statistics approach to epidemiology. *Sci. Rep.* **2020**, *10*, 19949. [CrossRef]
7. Şimşek, B.; Özilgen, M.; Utku, F.Ş. How much energy is stored in SARS-CoV-2 and its structural elements? *Energy Storage* **2022**, *4*, e298. [CrossRef]
8. Yilmaz, B.; Ercan, S.; Akduman, S.; Özilgen, M. Energetic and exergetic costs of COVID-19 infection on the body of a patient. *Int. J. Exergy* **2020**, *32*, 314–327. [CrossRef]
9. Popovic, M.; Martin, J.H.; Head, R.J. COVID infection in 4 steps: Thermodynamic considerations reveal how viral mucosal diffusion, target receptor affinity and furin cleavage act in concert to drive the nature and degree of infection in human COVID-19 disease. *Heliyon* **2023**, *9*, e17174. [CrossRef]
10. Gale, P. Thermodynamic equilibrium dose-response models for MERS-CoV infection reveal a potential protective role of human lung mucus but not for SARS-CoV-2. *Microb. Risk Anal.* **2020**, *16*, 100140. [CrossRef]
11. Popovic, M. Why doesn't Ebola virus cause pandemics like SARS-CoV-2? *Microb. Risk Anal.* **2022**, *22*, 100236. [CrossRef]
12. Casasnovas, J.M.; Springer, T.A. Kinetics and thermodynamics of virus binding to receptor: Studies with rhinovirus, intercellular adhesion molecule-1 (ICAM-1), and surface plasmon resonance. *J. Biol. Chem.* **1995**, *270*, 13216–13224. [CrossRef] [PubMed]
13. Popovic, M. Formulas for death and life: Chemical composition and biothermodynamic properties of Monkeypox (MPV, MPXV, HMPXV) and Vaccinia (VACV) viruses. *Therm. Sci.* **2022**, *26*, 4855–4868. [CrossRef]
14. Popović, M.E.; Šekularac, G.; Mihailović, M. Like a summer storm: Biothermodynamic analysis of Rotavirus A—Empirical formula, biosynthesis reaction and driving force of virus multiplication and antigen-receptor binding. *Microb. Risk Anal.* **2024**, *26*, 100291. [CrossRef]
15. Gale, P. How virus size and attachment parameters affect the temperature sensitivity of virus binding to host cells: Predictions of a thermodynamic model for arboviruses and HIV. *Microb. Risk Anal.* **2020**, *15*, 100104. [CrossRef] [PubMed]
16. Popović, M.E.; Stevanović, M.; Tadić, V. Biothermodynamic analysis of the Dengue virus: Empirical formulas, biosynthesis reactions and thermodynamic properties of antigen-receptor binding and biosynthesis. *Microb. Risk Anal.* **2024**, *27–28*, 100326. [CrossRef]
17. Popovic, M.; Popovic, M.; Šekularac, G. Death from the Nile: Empirical formula, molar mass, biosynthesis reaction and Gibbs energy of biosynthesis of the West Nile virus. *Microb. Risk Anal.* **2023**, *25*, 100281. [CrossRef]
18. Gale, P. Towards a thermodynamic mechanistic model for the effect of temperature on arthropod vector competence for transmission of arboviruses. *Microb. Risk Anal.* **2019**, *12*, 27–43. [CrossRef]
19. Gale, P. Using thermodynamic parameters to calibrate a mechanistic dose-response for infection of a host by a virus. *Microb. Risk Anal.* **2018**, *8*, 1–13. [CrossRef]
20. Popović, M.E.; Šekularac, G.M.; Tadić, V.M.; Pantović Pavlović, M.R. The silent assassin: Empirical formulas, molar masses, biosynthesis reactions, enthalpies, entropies and Gibbs energies of biosynthesis and Gibbs energies of binding of Coxsackieviruses A and B. *Therm. Sci.* **2024**, *28*, 4737–4757. [CrossRef]

21. Popović, M.E.; Šekularac, G.; Popović, M. The wind of change: Gibbs energy of binding and infectivity evolution of Omicron BA.2.86 Pirola, EG.5.1, XBB.1.16 Arcturus, CH.1.1 and BN.1 variants of SARS-CoV-2. *Microb. Risk Anal.* **2024**, *26*, 100290. [CrossRef]
22. Gale, P. Using thermodynamic equilibrium models to predict the effect of antiviral agents on infectivity: Theoretical application to SARS-CoV-2 and other viruses. *Microb. Risk Anal.* **2022**, *21*, 100198. [CrossRef] [PubMed]
23. Özilgen, M.; Yilmaz, B. COVID-19 disease causes an energy supply deficit in a patient. *Int. J. Energy Res.* **2021**, *45*, 1157–1160. [CrossRef] [PubMed]
24. Popović, M.; Stevanović, M.; Mihailović, M. Breaking news: Empirical formulas, molar masses, biosynthesis reactions, and thermodynamic properties of virus particles, biosynthesis and binding of Omicron JN.1 variant of SARS-CoV-2. *J. Serbian Chem. Soc.* **2024**, *89*, 305–320. [CrossRef]
25. Popovic, M.; Pantović Pavlović, M.; Pavlović, M. Ghosts of the past: Elemental composition, biosynthesis reactions and thermodynamic properties of Zeta P.2, Eta B.1.525, Theta P.3, Kappa B.1.617.1, Iota B.1.526, Lambda C.37 and Mu B.1.621 variants of SARS-CoV-2. *Microb. Risk Anal.* **2023**, *24*, 100263. [CrossRef]
26. Lucia, U.; Deisboeck, T.S.; Grisolia, G. Entropy-based pandemics forecasting. *Front. Phys.* **2020**, *8*, 274. [CrossRef]
27. Villarreal, L.P. Are viruses alive? *Sci. Am.* **2004**, *291*, 100–105. Available online: https://www.jstor.org/stable/26060805 (accessed on 4 May 2025). [CrossRef]
28. Moreno-Altamirano, M.M.B.; Kolstoe, S.E.; Sánchez-García, F.J. Virus control of cell metabolism for replication and evasion of host immune responses. *Front. Cell. Infect. Microbiol.* **2019**, *9*, 95. [CrossRef]
29. Eisenreich, W.; Rudel, T.; Heesemann, J.; Goebel, W. How viral and intracellular bacterial pathogens reprogram the metabolism of host cells to allow their intracellular replication. *Front. Cell. Infect. Microbiol.* **2019**, *9*, 42. [CrossRef]
30. Sankaran, N.; Weiss, R.A. Viruses: Impact on Science and Society. *Encycl. Virol.* **2021**, *1*, 671–680. [CrossRef]
31. Burrell, C.J.; Howard, C.R.; Murphy, F.A. History and Impact of Virology. *Fenner White's Med. Virol.* **2017**, 3–14. [CrossRef]
32. Zuo, K.; Gao, W.; Wu, Z.; Zhang, L.; Wang, J.; Yuan, X.; Li, C.; Xiang, Q.; Lu, L.; Liu, H. Evolution of Virology: Science History through Milestones and Technological Advancements. *Viruses* **2024**, *16*, 374. [CrossRef] [PubMed]
33. Enquist, L.W. Editors of the Journal of Virology Virology in the 21st century. *J. Virol.* **2009**, *83*, 5296–5308. [CrossRef] [PubMed]
34. Godfrey, S. A Review of *Virology: Molecular Biology and Pathogenesis*. *J. Microbiol. Biol. Educ. JMBE* **2011**, *12*, 213–214. [CrossRef]
35. Hartenian, E.; Nandakumar, D.; Lari, A.; Ly, M.; Tucker, J.M.; Glaunsinger, B.A. The molecular virology of coronaviruses. *J. Biol. Chem.* **2020**, *295*, 12910–12934. [CrossRef]
36. NCBI. NCBI Virus [Online] National Center for Biotechnology Information. 2024. Available online: https://www.ncbi.nlm.nih.gov/labs/virus/vssi/#/ (accessed on 3 August 2024).
37. Ritsch, M.; Cassman, N.A.; Saghaei, S.; Marz, M. Navigating the Landscape: A Comprehensive Review of Current Virus Databases. *Viruses* **2023**, *15*, 1834. [CrossRef]
38. Khare, S.; Gurry, C.; Freitas, L.; Schultz, M.B.; Bach, G.; Diallo, A.; Akite, N.; Ho, J.; Lee, R.T.; Yeo, W.; et al. GISAID's Role in Pandemic Response. *China CDC Wkly.* **2021**, *3*, 1049–1051. [CrossRef]
39. Acheson, N.H. *Fundamentals of Molecular Virology*; John Wiley & Sons: Hoboken, NJ, USA, 2011; ISBN 978-0-470-90059-8.
40. Cann, A. *Principles of Molecular Virology*; Academic Press: Amsterdam, The Netherlands, 2001; ISBN 978-0-121-58533-4.
41. Lostroh, P. *Molecular and Cellular Biology of Viruses*; Garland Science: New York, NY, USA, 2019; ISBN 978-0-815-34523-7.
42. Wimmer, E. The test-tube synthesis of a chemical called poliovirus. The simple synthesis of a virus has far-reaching societal implications. *EMBO Rep.* **2006**, *7*, S3–S9. [CrossRef]
43. Popović, M.E.; Pantović Pavlović, M.; Popović, M. Eris—Another brick in the wall: Empirical formulas, molar masses, biosynthesis reactions, enthalpy, entropy and Gibbs energy of Omicron EG.5 Eris and EG.5.1 variants of SARS-CoV-2. *Microb. Risk Anal.* **2023**, *25*, 100280. [CrossRef]
44. Sanchez, E.L.; Lagunoff, M. Viral activation of cellular metabolism. *Virology* **2015**, *479–480*, 609–618. [CrossRef]
45. Polcicova, K.; Badurova, L.; Tomaskova, J. Metabolic reprogramming as a feast for virus replication. *Acta Virol.* **2020**, *64*, 201–215. [CrossRef]
46. Goyal, P.; Rajala, M.S. Reprogramming of glucose metabolism in virus infected cells. *Mol Cell Biochem* **2023**, *478*, 2409–2418. [CrossRef] [PubMed]
47. Louten, J. Virus Replication. *Essent. Hum. Virol.* **2016**, 49–70. [CrossRef]
48. Nagy, P.; Pogany, J. The dependence of viral RNA replication on co-opted host factors. *Nat Rev Microbiol* **2012**, *10*, 137–149. [CrossRef]
49. Chinchar, V.G. Replication of viruses. *Encycl. Virol.* **1999**, 1471–1478. [CrossRef]
50. Buzón, P.; Maity, S.; Christodoulis, P.; Wiertsema, M.J.; Dunkelbarger, S.; Kim, C.; Wuite, G.J.L.; Zlotnick, A.; Roos, W.H. Virus self-assembly proceeds through contact-rich energy minima. *Sci. Adv.* **2021**, *7*, eabg0811. [CrossRef]
51. Lawton, J.A.; Estes, M.K.; Prasad, B.V. Mechanism of genome transcription in segmented dsRNA viruses. *Adv. Virus Res.* **2000**, *55*, 185–229. [CrossRef]

52. Walsh, D.; Mathews, M.B.; Mohr, I. Tinkering with translation: Protein synthesis in virus-infected cells. *Cold Spring Harb. Perspect. Biol.* **2013**, *5*, a012351. [CrossRef]
53. Von Stockar, U. Live cells as open non-equilibrium systems. In *Biothermodynamics: The Role of Thermodynamics in Biochemical Engineering*; von Stockar, U., Ed.; EPFL Press: Lausanne, Switzerland, 2013; pp. 475–534. [CrossRef]
54. Demirel, Y. *Nonequilibrium Thermodynamics: Transport and Rate Processes in Physical, Chemical and Biological Systems*, 3rd ed.; Elsevier: Amsterdam, The Netherlands, 2014; ISBN 978-0-444-59581-2.
55. Sandler, S.I. *Chemical, Biochemical, and Engineering Thermodynamics*, 5th ed.; Wiley: Hoboken, NJ, USA, 2017; ISBN 978-0-470-50479-6.
56. Bar-Even, A.; Flamholz, A.; Noor, E.; Milo, R. Thermodynamic constraints shape the structure of carbon fixation pathways. *Biochim. Biophys. Acta* **2012**, *1817*, 1646–1659. [CrossRef]
57. Yang, X.; Heinemann, M.; Howard, J.; Huber, G.; Iyer-Biswas, S.; Le Treut, G.; Lynch, M.; Montooth, K.L.; Needleman, D.J.; Pigolotti, S.; et al. Physical bioenergetics: Energy fluxes, budgets, and constraints in cells. *Proc. Natl. Acad. Sci. USA* **2021**, *118*, e2026786118. [CrossRef]
58. Taha, A.; Patón, M.; Penas, D.R.; Banga, J.R.; Rodríguez, J. Optimal evaluation of energy yield and driving force in microbial metabolic pathway variants. *PLoS Comput. Biol.* **2023**, *19*, e1011264. [CrossRef]
59. Popovic, M. Atom counting method for determining elemental composition of viruses and its applications in biothermodynamics and environmental science. *Comput. Biol. Chem.* **2022**, *96*, 107621. [CrossRef] [PubMed]
60. Popović, M.; Popović, M.; Šekularac, G.; Pantović Pavlović, M. Omicron BA.2.86 Pirola nightmare: Empirical formulas and thermodynamic properties (enthalpy, entropy and Gibbs energy) of nucleocapsid, virus particle and biosynthesis of BA.2.86 Pirola variant of SARS-CoV-2. *J. Serbian Chem. Soc.* **2024**, *89*, 807–822. [CrossRef]
61. Head, R.J.; Popovic, M.; Martin, J.H. Has the human biological interaction with SARS-CoV2 variants entered a pliant "Faustian bargain"? *Pharmacol. Res. Perspect.* **2024**, *12*, e1244. [CrossRef] [PubMed]
62. Head, R.J.; Lumbers, E.R.; Jarrott, B.; Tretter, F.; Smith, G.; Pringle, K.G.; Islam, S.; Martin, J.H. Systems analysis shows that thermodynamic physiological and pharmacological fundamentals drive COVID-19 and response to treatment. *Pharmacol. Res. Perspect.* **2022**, *10*, e00922. [CrossRef] [PubMed]
63. Katen, S.; Zlotnick, A. The thermodynamics of virus capsid assembly. *Methods Enzymol.* **2009**, *455*, 395–417. [CrossRef]
64. Bruinsma, R.F.; Gelbart, W.M.; Reguera, D.; Rudnick, J.; Zandi, R. Viral self-assembly as a thermodynamic process. *Phys. Rev. Lett.* **2003**, *90*, 248101. [CrossRef]
65. Alexander, C.G.; Jürgens, M.C.; Shepherd, D.A.; Freund, S.M.; Ashcroft, A.E.; Ferguson, N. Thermodynamic origins of protein folding, allostery, and capsid formation in the human hepatitis B virus core protein. *Proc. Natl. Acad. Sci. USA* **2013**, *110*, E2782–E2791. [CrossRef]
66. Popović, M.E.; Pantović Pavlović, M.; Šekularac, G. Chemical and thermodynamic properties of *Bombyx mori* (domestic silk moth): Empirical formula, driving force, and biosynthesis, catabolism and metabolism reactions. *Therm. Sci.* **2023**, *27*, 4893–4910. [CrossRef]
67. Popovic, M. Strain Wars 5: Gibbs energies of binding of BA.1 through BA.4 variants of SARS-CoV-2. *Microb. Risk Anal.* **2022**, *22*, 100231. [CrossRef]
68. Skene, K.R. Systems theory, thermodynamics and life: Integrated thinking across ecology, organization and biological evolution. *Bio Syst.* **2024**, *236*, 105123. [CrossRef]
69. Skene, K.R. Life's a Gas: A Thermodynamic Theory of Biological Evolution. *Entropy* **2015**, *17*, 5522–5548. [CrossRef]
70. Popovic, M.E.; Mihailović, M.; Pavlović, S. Upcoming epidemic storm: Empirical formulas, biosynthesis reactions, thermodynamic properties and driving forces of multiplication of the omicron XBB.1.9.1, XBF and XBB.1.16 (Arcturus) variants of SARS-CoV-2. *Microb. Risk Anal.* **2023**, *25*, 100273. [CrossRef]
71. Popovic, M. Omicron BA.2.75 subvariant of SARS-CoV-2 is expected to have the greatest infectivity compared with the competing BA.2 and BA.5, due to most negative Gibbs energy of binding. *BioTech* **2022**, *11*, 45. [CrossRef]
72. Robilotti, E.; Deresinski, S.; Pinsky, B.A. Norovirus. *Clin. Microbiol. Rev.* **2015**, *28*, 134–164. [CrossRef]
73. Desselberger, U. *Caliciviridae* Other Than Noroviruses. *Viruses* **2019**, *11*, 286. [CrossRef]
74. Greer, A.L.; Drews, S.J.; Fisman, D.N. Why "Winter" Vomiting Disease? Seasonality, Hydrology, and Norovirus Epidemiology in Toronto, Canada. *EcoHealth* **2009**, *6*, 192–199. [CrossRef]
75. Kirby, A.E.; Streby, A.; Moe, C.L. Vomiting as a Symptom and Transmission Risk in Norovirus Illness: Evidence from Human Challenge Studies. *PLoS ONE* **2016**, *11*, e0143759. [CrossRef]
76. Tan, M.; Tian, Y.; Zhang, D.; Wang, Q.; Gao, Z. Aerosol Transmission of Norovirus. *Viruses* **2024**, *16*, 151. [CrossRef]
77. Randazzo, W.; D'Souza, D.H.; Sanchez, G. Norovirus: The Burden of the Unknown. *Adv. Food Nutr. Res.* **2018**, *86*, 13–53. [CrossRef]
78. Carlson, K.B.; Dilley, A.; O'Grady, T.; Johnson, J.A.; Lopman, B.; Viscidi, E. A narrative review of norovirus epidemiology, biology, and challenges to vaccine development. *NPJ Vaccines* **2024**, *9*, 94. [CrossRef]

79. Capece, G.; Gignac, E. Norovirus. [Updated 14 August 2023]. In *StatPearls [Internet]*; StatPearls Publishing: Treasure Island, FL, USA, 2024. Available online: https://www.ncbi.nlm.nih.gov/books/NBK513265/ (accessed on 30 January 2024).
80. Hall, A.J. Noroviruses: The perfect human pathogens? *J. Infect. Dis.* **2012**, *205*, 1622–1624. [CrossRef] [PubMed]
81. Esposito, S.; Ascolese, B.; Senatore, L.; Codecà, C. Pediatric norovirus infection. *Eur. J. Clin. Microbiol. Infect. Dis.* **2014**, *33*, 285–290. [CrossRef] [PubMed]
82. Barclay, L.; Park, G.W.; Vega, E.; Hall, A.; Parashar, U.; Vinjé, J.; Lopman, B. Infection control for norovirus. *Clin. Microbiol. Infect. Off. Publ. Eur. Soc. Clin. Microbiol. Infect. Dis.* **2014**, *20*, 731–740. [CrossRef] [PubMed]
83. Overbey, K.N.; Hamra, G.B.; Nachman, K.E.; Rock, C.; Schwab, K.J. Quantitative microbial risk assessment of human norovirus infection in environmental service workers due to healthcare-associated fomites. *J. Hosp. Infect.* **2021**, *117*, 52–64. [CrossRef]
84. CDC. About Norovirus [Online], U.S. Centers for Disease Control and Prevention. 2024. Available online: https://www.cdc.gov/norovirus/about/index.html (accessed on 8 June 2024).
85. HSA Norovirus: What to Do If You Catch It and Helping to Stop the Spread [Online] United Kingdom Health Security Agency. 2024. Available online: https://ukhsa.blog.gov.uk/2022/11/17/norovirus-what-to-do-if-you-catch-it-and-helping-to-stop-the-spread/ (accessed on 8 June 2024).
86. Winder, N.; Gohar, S.; Muthana, M. Norovirus: An Overview of Virology and Preventative Measures. *Viruses* **2022**, *14*, 2811. [CrossRef]
87. Yunus, M.A. Molecular Mechanisms for Norovirus Genome Replication. *IntechOpen* **2021**. [CrossRef]
88. Modrow, S.; Falke, D.; Truyen, U.; Schätzl, H. Viruses with Single-Stranded, Positive-Sense RNA Genomes. *Mol. Virol.* **2013**, 185–349. [CrossRef]
89. Ryu, W.S. Other Positive-Strand RNA Viruses. *Mol. Virol. Hum. Pathog. Viruses* **2017**, 177–184. [CrossRef]
90. Rani, M.; Rajyalakshmi, S.; Pakalapaty, S.; Kammilli, N. Norovirus Structure and Classification. *IntechOpen* **2021**. [CrossRef]
91. Graziano, V.R.; Wei, J.; Wilen, C.B. Norovirus Attachment and Entry. *Viruses* **2019**, *11*, 495. [CrossRef]
92. Song, C.; Takai-Todaka, R.; Miki, M.; Haga, K.; Fujimoto, A.; Ishiyama, R.; Oikawa, K.; Yokoyama, M.; Miyazaki, N.; Iwasaki, K.; et al. Dynamic rotation of the protruding domain enhances the infectivity of norovirus. *PLoS Pathog.* **2020**, *16*, e1008619. [CrossRef] [PubMed]
93. Liu, W.; Chen, Y.; Jiang, X.; Xia, M.; Yang, Y.; Tan, M.; Li, X.; Rao, Z. A Unique Human Norovirus Lineage with a Distinct HBGA Binding Interface. *PLoS Pathog.* **2015**, *11*, e1005025. [CrossRef] [PubMed]
94. Pogan, R.; Weiss, V.U.; Bond, K.; Dülfer, J.; Krisp, C.; Lyktey, N.; Müller-Guhl, J.; Zoratto, S.; Allmaier, G.; Jarrold, M.F.; et al. N-terminal VP1 Truncations Favor $T = 1$ Norovirus-Like Particles. *Vaccines* **2020**, *9*, 8. [CrossRef] [PubMed]
95. Hu, L.; Salmen, W.; Chen, R.; Zhou, Y.; Neill, F.; Crowe, J.E.; Jr Atmar, R.L.; Estes, M.K.; Prasad, B.V.V. Atomic structure of the predominant GII.4 human norovirus capsid reveals novel stability and plasticity. *Nat. Commun.* **2022**, *13*, 1241. [CrossRef]
96. Prasad, B.V.; Schmid, M.F. Principles of virus structural organization. *Adv. Exp. Med. Biol.* **2012**, *726*, 17–47. [CrossRef]
97. Venkataram Prasad, B.V.; Shanker, S.; Muhaxhiri, Z.; Choi, J.M.; Atmar, R.L.; Estes, M.K. Structural Biology of Noroviruses. *Viral Gastroenteritis* **2016**, 329–354. [CrossRef]
98. Smith, H.Q.; Smith, T.J. The Dynamic Capsid Structures of the Noroviruses. *Viruses* **2019**, *11*, 235. [CrossRef]
99. Devant, J.M.; Hansman, G.S. Structural heterogeneity of a human norovirus vaccine candidate. *Virology* **2021**, *553*, 23–34. [CrossRef]
100. Devant, J.M.; Hofhaus, G.; Bhella, D.; Hansman, G.S. Heterologous expression of human norovirus GII.4 VP1 leads to assembly of T=4 virus-like particles. *Antivir. Res.* **2019**, *168*, 175–182. [CrossRef]
101. Hardy, M.E. Norovirus protein structure and function. *FEMS Microbiol. Lett.* **2005**, *253*, 1–8. [CrossRef]
102. Jung, J.; Grant, T.; Thomas, D.R.; Diehnelt, C.W.; Grigorieff, N.; Joshua-Tor, L. High-resolution cryo-EM structures of outbreak strain human norovirus shells reveal size variations. *Proc. Natl. Acad. Sci. USA* **2019**, *116*, 12828–12832. [CrossRef] [PubMed]
103. Creutznacher, R.; Maass, T.; Dülfer, J.; Feldmann, C.; Hartmann, V.; Lane, M.S.; Knickmann, J.; Westermann, L.T.; Thiede, L.; Smith, T.J.; et al. Distinct dissociation rates of murine and human norovirus P-domain dimers suggest a role of dimer stability in virus-host interactions. *Commun. Biol.* **2022**, *5*, 563. [CrossRef] [PubMed]
104. Tubiana, T.; Boulard, Y.; Bressanelli, S. Dynamics and asymmetry in the dimer of the norovirus major capsid protein. *PLoS ONE* **2017**, *12*, e0182056. [CrossRef] [PubMed]
105. Tan, M.; Jiang, X. The p domain of norovirus capsid protein forms a subviral particle that binds to histo-blood group antigen receptors. *J. Virol.* **2005**, *79*, 14017–14030. [CrossRef]
106. Tan, M.; Hegde, R.S.; Jiang, X. The P domain of norovirus capsid protein forms dimer and binds to histo-blood group antigen receptors. *J. Virol.* **2004**, *78*, 6233–6242. [CrossRef]
107. Vongpunsawad, S.; Venkataram Prasad, B.V.; Estes, M.K. Norwalk Virus Minor Capsid Protein VP2 Associates within the VP1 Shell Domain. *J. Virol.* **2013**, *87*, 4818–4825. [CrossRef]
108. Snowden, J.S.; Hurdiss, D.L.; Adeyemi, O.O.; Ranson, N.A.; Herod, M.R.; Stonehouse, N.J. Dynamics in the murine norovirus capsid revealed by high-resolution cryo-EM. *PLoS Biol.* **2020**, *18*, e3000649. [CrossRef]

109. Tan, M.; Jiang, X. Norovirus Capsid Protein-Derived Nanoparticles and Polymers as Versatile Platforms for Antigen Presentation and Vaccine Development. *Pharmaceutics* **2019**, *11*, 472. [CrossRef]
110. Strong, D.W.; Thackray, L.B.; Smith, T.J.; Virgin, H.W. Protruding domain of capsid protein is necessary and sufficient to determine murine norovirus replication and pathogenesis in vivo. *J. Virol.* **2012**, *86*, 2950–2958. [CrossRef]
111. Chen, Y.L.; Chang, P.J.; Huang, C.T. Small P particles formed by the Taiwan-native norovirus P domain overexpressed in *Komagataella pastoris*. *Appl. Microbiol. Biotechnol.* **2018**, *102*, 9707–9718. [CrossRef]
112. Campillay-Véliz, C.P.; Carvajal, J.J.; Avellaneda, A.M.; Escobar, D.; Covián, C.; Kalergis, A.M.; Lay, M.K. Human Norovirus Proteins: Implications in the Replicative Cycle, Pathogenesis, and the Host Immune Response. *Front. Immunol.* **2020**, *11*, 961. [CrossRef] [PubMed]
113. Lochridge, V.P.; Jutila, K.L.; Graff, J.W.; Hardy, M.E. Epitopes in the P2 domain of norovirus VP1 recognized by monoclonal antibodies that block cell interactions. *J. Gen. Virol.* **2005**, *86 Pt 1*, 2799–2806. [CrossRef] [PubMed]
114. Tan, M.; Huang, P.; Meller, J.; Zhong, W.; Farkas, T.; Jiang, X. Mutations within the P2 domain of norovirus capsid affect binding to human histo-blood group antigens: Evidence for a binding pocket. *J. Virol.* **2003**, *77*, 12562–12571. [CrossRef]
115. Cao, S.; Lou, Z.; Tan, M.; Chen, Y.; Liu, Y.; Zhang, Z.; Zhang, X.C.; Jiang, X.; Li, X.; Rao, Z. Structural basis for the recognition of blood group trisaccharides by norovirus. *J. Virol.* **2007**, *81*, 5949–5957. [CrossRef]
116. Ludwig-Begall, L.F.; Mauroy, A.; Thiry, E. Noroviruses-The State of the Art, Nearly Fifty Years after Their Initial Discovery. *Viruses* **2021**, *13*, 1541. [CrossRef]
117. Perry, J.W.; Wobus, C.E. Endocytosis of murine norovirus 1 into murine macrophages is dependent on dynamin II and cholesterol. *J. Virol.* **2010**, *84*, 6163–6176. [CrossRef]
118. Perry, J.W.; Taube, S.; Wobus, C.E. Murine norovirus-1 entry into permissive macrophages and dendritic cells is pH-independent. *Virus Res.* **2009**, *143*, 125–129. [CrossRef]
119. Le Pendu, J.; Rydell, G.E.; Nasir, W.; Larson, G. *Chapter 3.3—Human Norovirus Receptors*; Gastroenteritis, V., Svensson, L., Desselberger, U., Greenberg, H.B., Estes, M.K., Eds.; Academic Press: Amsterdam, The Netherlands, 2016. [CrossRef]
120. Sayers, E.W.; Bolton, E.E.; Brister, J.R.; Canese, K.; Chan, J.; Comeau, D.C.; Connor, R.; Funk, K.; Kelly, C.; Kim, S.; et al. Database resources of the national center for biotechnology information. *Nucleic Acids Res.* **2022**, *50*, D20–D26. [CrossRef]
121. NCBI NCBI Database [Online]. National Center for Biotechnology Information. 2024. Available online: https://www.ncbi.nlm.nih.gov/ (accessed on 24 May 2024).
122. NCBI NC_044932.1—Norovirus GII GII.NA2[PNA2], Complete Sequence [Online] National Center for Biotechnology Information. 2024. Available online: https://www.ncbi.nlm.nih.gov/nuccore/NC_044932.1 (accessed on 24 May 2024).
123. Tohma, K.; Saito, M.; Mayta, H.; Zimic, M.; Lepore, C.J.; Ford-Siltz, L.A.; Gilman, R.H.; Parra, G.I. Complete Genome Sequence of a Nontypeable GII Norovirus Detected in Peru. *Genome Announc.* **2018**, *6*, e00095-18. [CrossRef]
124. NCBI AIV43156—VP1, Norovirus GII.4 [Online] National Center for Biotechnology Information. 2024. Available online: https://www.ncbi.nlm.nih.gov/protein/AIV43156.2 (accessed on 24 May 2024).
125. Chan, M.C.; Lee, N.; Hung, T.N.; Kwok, K.; Cheung, K.; Tin, E.K.; Lai, R.W.; Nelson, E.A.; Leung, T.F.; Chan, P.K. Rapid emergence and predominance of a broadly recognizing and fast-evolving norovirus GII.17 variant in late 2014. *Nat. Commun.* **2015**, *6*, 10061. [CrossRef]
126. Prasad, B.V.; Hardy, M.E.; Dokland, T.; Bella, J.; Rossmann, M.G.; Estes, M.K. X-ray crystallographic structure of the Norwalk virus capsid. *Science* **1999**, *286*, 287–290. [CrossRef] [PubMed]
127. Tan, M.; Meller, J.; Jiang, X. C-terminal arginine cluster is essential for receptor binding of norovirus capsid protein. *J. Virol.* **2006**, *80*, 7322–7331. [CrossRef] [PubMed]
128. Nelson, C.A.; Wilen, C.B.; Dai, Y.N.; Orchard, R.C.; Kim, A.S.; Stegeman, R.A.; Hsieh, L.L.; Smith, T.J.; Virgin, H.W.; Fremont, D.H. Structural basis for murine norovirus engagement of bile acids and the CD300lf receptor. *Proc. Natl. Acad. Sci. USA* **2018**, *115*, E9201–E9210. [CrossRef] [PubMed]
129. Mills, J.T.; Minogue, S.C.; Snowden, J.S.; Arden, W.K.C.; Rowlands, D.J.; Stonehouse, N.J.; Wobus, C.E.; Herod, M.R. Amino acid substitutions in norovirus VP1 dictate cell tropism via an attachment process dependent on membrane mobility. *Biorxiv Prepr. Serv. Biol.* **2023**. [CrossRef]
130. Popovic, M.; Tadić, V.; Mihailović, M. From genotype to phenotype with biothermodynamics: Empirical formulas, biosynthesis reactions and thermodynamic properties of preproinsulin, proinsulin and insulin molecules. *J. Biomol. Struct. Dyn.* **2023**, *42*, 10388–10400. [CrossRef]
131. Popović, M.E.; Stevanović, M.; Pantović Pavlović, M. Biothermodynamics of hemoglobin and red blood cells: Analysis of structure and evolution of hemoglobin and red blood cells, based on molecular and empirical formulas, biosynthesis reactions, and thermodynamic properties of formation and biosynthesis. *J. Mol. Evol.* **2024**, *92*, 776–798. [CrossRef]
132. Popović, M.E.; Popović, M.; Pei, D. Biothermodynamic Analysis of *Caenorhabditis elegans*: Model of Growth and Metabolism Based on Empirical Formulas, Metabolism Reactions, and Thermodynamic Properties of Living Matter and Metabolism. *Biophysica* **2025**, *5*, 19. [CrossRef]

133. Patel, S.A.; Erickson, L.E. Estimation of heats of combustion of biomass from elemental analysis using available electron concepts. *Biotechnol. Bioeng.* **1981**, *23*, 2051–2067. [CrossRef]
134. Battley, E.H. The development of direct and indirect methods for the study of the thermodynamics of microbial growth. *Thermochim. Acta* **1998**, *309*, 17–37. [CrossRef]
135. Popovic, M. Animal bioenergetics: Thermodynamic and kinetic analysis of growth and metabolism of Anguilla anguilla. *Zoology* **2024**, *163*, 126158. [CrossRef]
136. Grisolia, G.; Fino, D.; Lucia, U. Thermodynamic optimisation of the biofuel production based on mutualism. *Energy Rep.* **2020**, *6*, 1561–1571. [CrossRef]
137. Grisolia, G.; Fino, D.; Lucia, U. Biomethanation of rice straw: A sustainable perspective for the valorisation of a field residue in the energy sector. *Sustainability* **2022**, *14*, 5679. [CrossRef]
138. Barros, N.; Popovic, M.; Molina-Valero, J.; Lestido-Cardama, Y.; Pérez-Cruzado, C. Unravelling the thermodynamic properties of soil ecosystems in mature beech forests. *Sci. Rep.* **2024**, *14*, 16644. [CrossRef] [PubMed]
139. Battley, E.H. The thermodynamics of microbial growth. In *Handbook of Thermal Analysis and Calorimetry, Vol. 4: From Macromolecules to Man*; Kemp, E.B., Ed.; Elsevier: Amsterdam, The Netherlands, 1999; pp. 219–235. [CrossRef]
140. Battley, E.H. On the enthalpy of formation of Escherichia coli K-12 cells. *Biotechnol. Bioeng.* **1992**, *39*, 5–12. [CrossRef]
141. Thornton, W.M.X.V. The relation of oxygen to the heat of combustion of organic compounds. *Lond. Edinb. Dublin Philos. Mag. J. Sci.* **1917**, *33*, 196–203. [CrossRef]
142. Battley, E.H. An empirical method for estimating the entropy of formation and the absolute entropy of dried microbial biomass for use in studies on the thermodynamics of microbial growth. *Thermochim. Acta* **1999**, *326*, 7–15. [CrossRef]
143. Battley, E.H.; Stone, J.R. A comparison of values for the entropy and the entropy of formation of selected organic substances of biological importance in the solid state, as determined experimentally or calculated empirically. *Thermochim. Acta* **2000**, *349*, 153–161. [CrossRef]
144. Atkins, P.W.; de Paula, J. *Physical Chemistry for the Life Sciences*, 2nd ed.; W.H. Freeman and Company: New York, NY, USA, 2011; ISBN 978-1-429-23114-5.
145. Atkins, P.W.; de Paula, J. *Physical Chemistry: Thermodynamics, Structure, and Change*, 10th ed.; W.H. Freeman and Company: New York, NY, USA, 2014; ISBN 978-1-429-29019-7.
146. Özilgen, M. Review on biothermoydnamics applications: Timeline, challenges, and opportunities. *Int. J. Energy Res.* **2017**, *41*, 1513–1533. [CrossRef]
147. Brown, T.; LeMay, H.; Bursten, B.; Murphy, C.; Woodward, P.; Stoltzfus, M. *Chemistry: The Central Science*, 14th ed.; Pearson: London, UK, 2017; ISBN 978-0-134-41423-2.
148. McMurry, J.; Ballantine, D.; Hoeger, C.; Peterson, V. *Fundamentals of General, Organic, and Biological Chemistry (MasteringChemistry)*, 8th ed.; Pearson: London, UK, 2016.
149. Assael, M.J.; Maitland, G.C.; Maskow, T.; von Stockar, U.; Wakeham, W.A.; Will, S. *Commonly Asked Questions in Thermodynamics*, 2nd ed.; CRC Press: Boca Raton, FL, USA, 2022; ISBN 978-0-367-33891-6. [CrossRef]
150. Von Stockar, U. Biothermodynamics of live cells: Energy dissipation and heat generation in cellular structures. In *Biothermodynamics: The role of thermodynamics in Biochemical Engineering*; von Stockar, U., Ed.; EPFL Press: Lausanne, Switzerland, 2013; pp. 475–534. [CrossRef]
151. von Stockar, U. The role of thermodynamics in biochemical engineering. *J. Non Equilib. Thermodyn.* **2013**, *38*, 225–240. [CrossRef]
152. Battley, E.H. Calculation of thermodynamic properties of protein in Escherichia coli K-12 grown on succinic acid, energy changes accompanying protein anabolism, and energetic role of ATP in protein synthesis. *Biotechnol. Bioeng.* **1992**, *40*, 280–288. [CrossRef]
153. Popovic, M. XBB.1.5 Kraken cracked: Gibbs energies of binding and biosynthesis of the XBB.1.5 variant of SARS-CoV-2. *Microbiol. Res.* **2023**, *270*, 127337. [CrossRef] [PubMed]
154. Popovic, M. The SARS-CoV-2 Hydra, a monster from the 21st century: Thermodynamics of the BA.5.2 and BF.7 variants. *Microb. Risk Anal.* **2023**, *23*, 100249. [CrossRef] [PubMed]
155. Popovic, M. SARS-CoV-2 strain wars continues: Chemical and thermodynamic characterization of live matter and biosynthesis of Omicron BN.1, CH.1.1 and XBC variants. *Microb. Risk Anal.* **2023**, *24*, 100260. [CrossRef] [PubMed]
156. Battley, E.H. A comparison of energy changes accompanying growth processes by Saccharomyces cerevisiae. *J. Therm. Anal. Calorim.* **2011**, *104*, 193–200. [CrossRef]
157. Battley, E.H. The sources of thermal energy exchange accompanying microbial anabolism. *J. Therm. Anal. Calorim.* **2007**, *87*, 105–111. [CrossRef]
158. Semercioöz, A.S.; Soyalp, K.; Ulu, G.; Özilgen, M. Effects of energy storage by the seaweeds on their ecosystem. *Energy Storage* **2021**, *3*, e266. [CrossRef]
159. Sorgüven, E.; Özilgen, M. Energy utilization, carbon dioxide emission, and exergy loss in flavored yogurt production process. *Energy* **2012**, *40*, 214–225. [CrossRef]

160. Lucia, U.; Fino, D.; Wensel, P.; Grisolia, G. Thermodynamic approach to biofuels from microalgae and cyanobacteria: The role of electrochemical potential. *Atti Della Accad. Peloritana Pericolanti Cl. Sci. Fis. Mat. E Nat.* **2022**, *100*, 1. [CrossRef]
161. Riedel, S.; Hobden, J.A.; Miller, S.; Morse, S.A.; Mietzner, T.A.; Detrick, B.; Mitchell, T.G.; Sakanari, J.A.; Hotez, P.; Mejia, R. *Jawetz, Melnick and Adelberg's Medical Microbiology*, 28th ed.; McGraw-Hill: New York, NY, USA, 2019; ISBN 978-1-260-01202-6.
162. Du, X.; Li, Y.; Xia, Y.L.; Ai, S.M.; Liang, J.; Sang, P.; Ji, X.L.; Liu, S.Q. Insights into Protein-Ligand Interactions: Mechanisms, Models, and Methods. *Int. J. Mol. Sci.* **2016**, *17*, 144. [CrossRef]
163. Rusnati, M.; Chiodelli, P.; Bugatti, A.; Urbinati, C. Bridging the past and the future of virology: Surface plasmon resonance as a powerful tool to investigate virus/host interactions. *Crit. Rev. Microbiol.* **2015**, *41*, 238–260. [CrossRef]
164. Beatty, J.D.; Beatty, B.G.; Vlahos, W.G. Measurement of monoclonal antibody affinity by non-competitive enzyme immunoassay. *J. Immunol. Methods* **1987**, *100*, 173–179. [CrossRef] [PubMed]
165. Karst, S.M.; Wobus, C.E. A working model of how noroviruses infect the intestine. *PLoS Pathog.* **2015**, *11*, e1004626. [CrossRef] [PubMed]
166. Gelderblom, H.R. Structure and Classification of Viruses. In *Medical Microbiology*, 4th ed.; Baron, S., Ed.; University of Texas Medical Branch at Galveston: Galveston, TX, USA, 1996.
167. Summers, W.C. Virus Infection. *Encycl. Microbiol.* **2009**, 546–552. [CrossRef]
168. Davey, N.E.; Travé, G.; Gibson, T.J. How viruses hijack cell regulation. *Trends Biochem. Sci.* **2011**, *36*, 159–169. [CrossRef]
169. Thaker, S.K.; Ch'ng, J.; Christofk, H.R. Viral hijacking of cellular metabolism. *BMC Biol.* **2019**, *17*, 59. [CrossRef]
170. Girdhar, K.; Powis, A.; Raisingani, A.; Chrudinová, M.; Huang, R.; Tran, T.; Sevgi, K.; Dogus Dogru, Y.; Altindis, E. Viruses and Metabolism: The Effects of Viral Infections and Viral Insulins on Host Metabolism. *Annu. Rev. Virol.* **2021**, *8*, 373–391. [CrossRef]
171. Mayer, K.A.; Stöckl, J.; Zlabinger, G.J.; Gualdoni, G.A. Hijacking the Supplies: Metabolism as a Novel Facet of Virus-Host Interaction. *Front. Immunol.* **2019**, *10*, 1533. [CrossRef]
172. Goodwin, C.M.; Xu, S.; Munger, J. Stealing the Keys to the Kitchen: Viral Manipulation of the Host Cell Metabolic Network. *Trends Microbiol.* **2015**, *23*, 789–798. [CrossRef]
173. Popovic, M. Biothermodynamics of Viruses from Absolute Zero (1950) To—Virothermodynamics (2022). *Vaccines* **2022**, *10*, 2112. [CrossRef]
174. Popovic, M. Omicron BA.2.75 Sublineage (Centaurus) Follows the Expectations of the Evolution Theory: Less Negative Gibbs Energy of Biosynthesis Indicates Decreased Pathogenicity. *Microbiol. Res.* **2022**, *13*, 937–952. [CrossRef]
175. Popovic, M. Comparative study of entropy and information change in closed and open thermodynamic systems. *Thermochim. Acta* **2014**, *598*, 77–81. [CrossRef]
176. Popovic, M.; Stenning, G.B.; Göttlein, A.; Minceva, M. Elemental composition, heat capacity from 2 to 300 K and derived thermodynamic functions of 5 microorganism species. *J. Biotechnol.* **2021**, *331*, 99–107. [CrossRef] [PubMed]
177. Balmer, R.T. *Modern Engineering Thermodynamics*; Academic Press: Cambridge, MA, USA, 2010. [CrossRef]
178. Ozilgen, M.; Sorguven Oner, E. *Biothermodynamics: Principles and Applications*, 1st ed.; CRC Press: Boca Raton, FL, USA, 2016. [CrossRef]
179. Popovic, M. Never ending story? Evolution of SARS-CoV-2 monitored through Gibbs energies of biosynthesis and antigen-receptor binding of Omicron BQ.1, BQ.1.1, XBB and XBB.1 variants. *Microb. Risk Anal.* **2023**, *23*, 100250. [CrossRef] [PubMed]
180. von Stockar, U. Biothermodynamics of live cells: A tool for biotechnology and biochemical engineering. *J. Non Equilib. Thermodyn.* **2010**, *35*, 415–475. [CrossRef]
181. Von Stockar, U.; Maskow, T.; Liu, J.; Marison, I.W.; Patino, R. Thermodynamics of microbial growth and metabolism: An analysis of the current situation. *J. Biotechnol.* **2006**, *121*, 517–533. [CrossRef] [PubMed]
182. Von Stockar, U.; van der Wielen, L.A. Thermodynamics in biochemical engineering. *J. Biotechnol.* **1997**, *59*, 25–37. [CrossRef]
183. Chu, P.Y.; Huang, H.W.; Boonchan, M.; Tyan, Y.C.; Louis, K.L.; Lee, K.M.; Motomura, K.; Ke, L.Y. Mass Spectrometry-Based System for Identifying and Typing Norovirus Major Capsid Protein VP1. *Viruses* **2021**, *13*, 2332. [CrossRef]
184. Feng, K.; Divers, E.; Ma, Y.; Li, J. Inactivation of a human norovirus surrogate, human norovirus virus-like particles, and vesicular stomatitis virus by gamma irradiation. *Appl. Environ. Microbiol.* **2011**, *77*, 3507–3517. [CrossRef]
185. Molla, A.; Paul, A.V.; Wimmer, E. Cell-free, de novo synthesis of poliovirus. *Science* **1991**, *254*, 1647–1651. [CrossRef]
186. Mehndiratta, M.M.; Mehndiratta, P.; Pande, R. Poliomyelitis: Historical facts, epidemiology, and current challenges in eradication. *Neurohospitalist* **2014**, *4*, 223–229. [CrossRef]
187. Kapikian, A.Z.; Shope, R.E. Rotaviruses, Reoviruses, Coltiviruses, and Orbiviruses. In *Medical Microbiology*, 4th ed.; Baron, S., Ed.; University of Texas Medical Branch at Galveston: Galveston, TX, USA, 1996; Chapter 63. Available online: https://www.ncbi.nlm.nih.gov/books/NBK8558/ (accessed on 4 May 2025).
188. Martín-Acebes, M.A.; Saiz, J.C. West Nile virus: A re-emerging pathogen revisited. *World J. Virol.* **2012**, *1*, 51–70. [CrossRef] [PubMed]

189. Azuma, K.; Yanagi, U.; Kagi, N.; Kim, H.; Ogata, M.; Hayashi, M. Environmental factors involved in SARS-CoV-2 transmission: Effect and role of indoor environmental quality in the strategy for COVID-19 infection control. *Environ. Health Prev. Med.* **2020**, *25*, 66. [CrossRef] [PubMed]
190. Chan, M.C.W.; Shan Kwan, H.; Chan, P.K.S. Structure and Genotypes of Noroviruses. *Norovirus* **2017**, 51–63. [CrossRef]
191. Degueldre, C. Single virus inductively coupled plasma mass spectroscopy analysis: A comprehensive study. *Talanta* **2021**, *228*, 122211. [CrossRef]
192. Popovic, M.; Šekularac, G.; Stevanović, M. Thermodynamics of microbial consortia: Enthalpies and Gibbs energies of microorganism live matter and macromolecules of *E. coli*, *G. oxydans*, *P. fluorescens*, *S. thermophilus* and *P. chrysogenum*. *J. Biotechnol.* **2024**, *379*, 6–17. [CrossRef]
193. Battley, E.H. A theoretical study of the thermodynamics of microbial growth using Saccharomyces cerevisiae and a different free energy equation. *Q. Rev. Biol.* **2013**, *88*, 69–96. [CrossRef]
194. Karst, S.M. Pathogenesis of noroviruses, emerging RNA viruses. *Viruses* **2010**, *2*, 748–781. [CrossRef]
195. Mateu, M.G. Introduction: The structural basis of virus function. *Sub Cell. Biochem.* **2013**, *68*, 3–51. [CrossRef]
196. Melano, I.; Kuo, L.L.; Lo, Y.C.; Sung, P.W.; Tien, N.; Su, W.C. Effects of Basic Amino Acids and Their Derivatives on SARS-CoV-2 and Influenza-A Virus Infection. *Viruses* **2021**, *13*, 1301. [CrossRef]
197. Payne, S. Virus Interactions With the Cell. *Viruses* **2017**, 23–35. [CrossRef]
198. Tyl, M.D.; Betsinger, C.N.; Cristea, I.M. Virus-host protein interactions as footprints of human cytomegalovirus replication. *Curr. Opin. Virol.* **2022**, *52*, 135–147. [CrossRef] [PubMed]
199. Zhang, D.; Ouyang, Q. Nonequilibrium Thermodynamics in Biochemical Systems and Its Application. *Entropy* **2021**, *23*, 271. [CrossRef] [PubMed]
200. von Stockar, U.; Liu, J. Does microbial life always feed on negative entropy? Thermodynamic analysis of microbial growth. *Biochim. Biophys. Acta* **1999**, *1412*, 191–211. [CrossRef]
201. Popović, M.E.; Stevanović, M.; Pantović Pavlović, M. Return of the forgotten nightmare: Bordetella pertussis uses a more negative Gibbs energy of metabolism to outcompete its host organism. *Microb. Risk Anal.* **2024**, *26*, 100292. [CrossRef]
202. Nagy, P.D.; Lin, W. Taking over Cellular Energy-Metabolism for TBSV Replication: The High ATP Requirement of an RNA Virus within the Viral Replication Organelle. *Viruses* **2020**, *12*, 56. [CrossRef] [PubMed] [PubMed Central]
203. Qin, C.; Xie, T.; Yeh WWSavas, A.C.; Feng, P. Metabolic Enzymes in Viral Infection and Host Innate Immunity. *Viruses* **2023**, *16*, 35. [CrossRef] [PubMed] [PubMed Central]
204. Bonora, M.; Patergnani, S.; Rimessi, A.; De Marchi, E.; Suski, J.M.; Bononi, A.; Giorgi, C.; Marchi, S.; Missiroli, S.; Poletti, F.; et al. ATP synthesis and storage. *Purinergic Signal.* **2012**, *8*, 343–357. [CrossRef]
205. Duponchel, S.; Fischer, M.G. Viva lavidaviruses! Five features of virophages that parasitize giant DNA viruses. *PLoS Pathog.* **2019**, *15*, e1007592. [CrossRef]
206. Roizman, B. Multiplication. In *Medical Microbiology*, 4th ed.; Baron, S., Ed.; University of Texas Medical Branch at Galveston: Galveston, TX, USA, 1996; Chapter 42. Available online: https://www.ncbi.nlm.nih.gov/books/NBK8181/ (accessed on 4 May 2025).
207. Faisst, S. Propagation of viruses | Animal. In *Encyclopedia of Virology*, 2nd ed.; Granoff, A., Webster, R.G., Eds.; Elsevier: Amsterdam, The Netherlands, 1999; pp. 1408–1413. Available online: https://www.sciencedirect.com/science/article/pii/B0122270304002363 (accessed on 4 May 2025).
208. Sai, L.; Sun, J.; Shao, L.; Chen, S.; Liu, H.; Ma, L. Epidemiology and clinical features of rotavirus and norovirus infection among children in Ji'nan, China. *Virol. J.* **2013**, *10*, 302. [CrossRef]
209. Rackoff, L.A.; Bok, K.; Green, K.Y.; Kapikian, A.Z. Epidemiology and evolution of rotaviruses and noroviruses from an archival WHO Global Study in Children (1976–79) with implications for vaccine design. *PLoS ONE* **2013**, *8*, e59394. [CrossRef]
210. Nirwati, H.; Donato, C.M.; Mawarti, Y.; Mulyani, N.S.; Ikram, A.; Aman, A.T.; Peppelenbosch, M.P.; Soenarto, Y.; Pan, Q.; Hakim, M.S. Norovirus and rotavirus infections in children less than five years of age hospitalized with acute gastroenteritis in Indonesia. *Arch Virol* **2019**, *164*, 1515–1525. [CrossRef] [PubMed]
211. Amimo, J.O.; Raev, S.A.; Chepngeno, J.; Mainga, A.O.; Guo, Y.; Saif, L.; Vlasova, A.N. Rotavirus Interactions With Host Intestinal Epithelial Cells. *Front. Immunol.* **2021**, *12*, 793841. [CrossRef] [PubMed]
212. Oluwatoyin Japhet, M.; Adeyemi Adesina, O.; Famurewa, O.; Svensson, L.; Nordgren, J. Molecular epidemiology of rotavirus and norovirus in Ile-Ife, Nigeria: High prevalence of G12P [8] rotavirus strains and detection of a rare norovirus genotype. *J. Med. Virol.* **2012**, *84*, 1489–1496. [CrossRef] [PubMed]
213. Cilli, A.; Luchs, A.; Morillo, S.G.; Costa, F.F.; Carmona, R.d.e.C.; Timenetsky, M.d.o.C. Characterization of rotavirus and norovirus strains: A 6-year study (2004–2009). *J. Pediatr.* **2011**, *87*, 445–449. [CrossRef]
214. Mousavi Nasab, S.D.; Sabahi, F.; Makvandi, M.; Mirab Samiee, S.; Nadji, S.A.; Ravanshad, M. Epidemiology of Rotavirus-Norovirus Co-Infection and Determination of Norovirus Genogrouping among Children with Acute Gastroenteritis in Tehran, Iran. *Iran. Biomed. J.* **2016**, *20*, 280–286. [CrossRef]

215. El Qazoui, M.; Oumzil, H.; Baassi, L.; Omari, N.E.; Sadki, K.; Amzazi, S.; Benhafid, M.; Aouad, R.E. Rotavirus and Norovirus infections among acute gastroenteritis children in Morocco. *BMC Infect. Dis.* **2014**, *14*, 300. [CrossRef]
216. Quee, F.A.; de Hoog, M.L.A.; Schuurman, R.; Bruijning-Verhagen, P. Community burden and transmission of acute gastroenteritis caused by norovirus and rotavirus in the Netherlands (RotaFam): A prospective household-based cohort study. *Lancet Infect. Dis.* **2020**, *20*, 598–606. [CrossRef]
217. Rönnelid, Y.; Bonkoungou, I.J.O.; Ouedraogo, N.; Barro, N.; Svensson, L.; Nordgren, J. Norovirus and rotavirus in children hospitalised with diarrhoea after rotavirus vaccine introduction in Burkina Faso. *Epidemiol. Infect.* **2020**, *148*, e245. [CrossRef]
218. Santiso-Bellón, C.; Randazzo, W.; Pérez-Cataluña, A.; Vila-Vicent, S.; Gozalbo-Rovira, R.; Muñoz, C.; Buesa, J.; Sanchez, G.; Rodríguez Díaz, J. Epidemiological Surveillance of Norovirus and Rotavirus in Sewage (2016–2017) in Valencia (Spain). *Microorganisms* **2020**, *8*, 458. [CrossRef]
219. Piedade, J.; Nordgren, J.; Esteves, F.; Esteves, A.; Teodósio, R.; Svensson, L.; Istrate, C. Molecular epidemiology and host genetics of norovirus and rotavirus infections in Portuguese elderly living in aged care homes. *J. Med. Virol.* **2019**, *91*, 1014–1021. [CrossRef]

Disclaimer/Publisher's Note: The statements, opinions and data contained in all publications are solely those of the individual author(s) and contributor(s) and not of MDPI and/or the editor(s). MDPI and/or the editor(s) disclaim responsibility for any injury to people or property resulting from any ideas, methods, instructions or products referred to in the content.